

Thesis on HEMP by Capt. Terry Chapman in 1973 with Fortran  
Computer Code in rear- See below pages-

See web sites: . <http://lagridcoalition.org>, & [www.facebook.com/lagridcoalition](http://www.facebook.com/lagridcoalition), for  
further "Electromagnetic Pulse" information sources and newer computer coding.

A COMPUTER CODE FOR  
HIGH ALTITUDE EMP

THESIS

GNE/PH/74-1

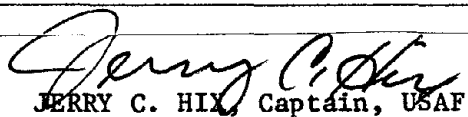
Terry C. Chapman  
Capt                      USAF

Approved for public release; distribution unlimited.



UNCLASSIFIED

SECURITY CLASSIFICATION OF THIS PAGE (When Data Entered)

REPORT DOCUMENTATION PAGE		READ INSTRUCTIONS BEFORE COMPLETING FORM
1. REPORT NUMBER GNE/PH/74-1	2. GOVT ACCESSION NO.	3. RECIPIENT'S CATALOG NUMBER AD 777841
4. TITLE (and Subtitle)  A COMPUTER CODE FOR HIGH ALTITUDE EMP		5. TYPE OF REPORT & PERIOD COVERED  THESIS
7. AUTHOR(s)  Terry C. Chapman, Captain, USAF		6. PERFORMING ORG. REPORT NUMBER
9. PERFORMING ORGANIZATION NAME AND ADDRESS AFIT/ENP Wright-Patterson AFB, OH 45433		8. CONTRACT OR GRANT NUMBER(s)
11. CONTROLLING OFFICE NAME AND ADDRESS AFIT/ENP Wright-Patterson AFB, OH 45433		10. PROGRAM ELEMENT, PROJECT, TASK AREA & WORK UNIT NUMBERS
14. MONITORING AGENCY NAME & ADDRESS (if different from Controlling Office) Air Force Weapons Laboratory/EL Kirtland AFB, New Mexico 87117		12. REPORT DATE January 1974
		13. NUMBER OF PAGES 82
		15. SECURITY CLASS. (of this report) UNCLASSIFIED
		15a. DECLASSIFICATION/DOWNGRADING SCHEDULE
16. DISTRIBUTION STATEMENT (of this Report)  Approved for public release; distribution unlimited		
17. DISTRIBUTION STATEMENT (of the abstract entered in Block 20, if different from Report)  PRICES SUBJECT TO CHANGE		
18. SUPPLEMENTARY NOTES  Approved for public release; IAW AFR 190-17.  <div style="text-align: right;">   JERRY C. HIX, Captain, USAF  Director of Information </div>		
19. KEY WORDS (Continue on reverse side if necessary and identify by block number) EMP High Altitude EMP EMP Computer Code  <div style="text-align: center;"> Reproduced by  NATIONAL TECHNICAL  INFORMATION SERVICE  U S Department of Commerce  Springfield VA 22151 </div>		
20. ABSTRACT (Continue on reverse side if necessary and identify by block number) A relatively inexpensive computer code is developed to calculate the peak value of the electric field contained in an electromagnetic pulse generated by the gamma rays from a high altitude nuclear burst. The code is based on the Karzas and Latter theory for the production of Compton electrons and their interaction with the earth's magnetic field. The code can be used to calculate the peak value of the electric field at a target anywhere on or above ground level.		

UNCLASSIFIED

SECURITY CLASSIFICATION OF THIS PAGE(When Data Entered)

20.

resulting from a nuclear burst above 60 km altitude with a gamma yield up to 60 tons. Either the direct or the ground reflected wave can be calculated. With special care, bursts up to 1 kt of gamma yield can be used.

UNCLASSIFIED

SECURITY CLASSIFICATION OF THIS PAGE(When Data Entered)

A COMPUTER CODE FOR  
HIGH ALTITUDE EMP

THESIS

Presented to the Faculty of the School of Engineering  
of the Air Force Institute of Technology  
Air University  
in Partial Fulfillment of the  
Requirements for the Degree of  
Master of Science

by

Terry C. Chapman, B.S.  
Capt                      USAF  
Graduate Nuclear Engineering

January 1974

Approved for public release; distribution unlimited.

ic

## Preface

It is my pleasure to recognize several people who contributed in various ways to make this work possible.

I want to thank my advisor, Maj Carl T. Case. His patience and helpful suggestions were important factors to the successful conclusion of this work. In addition, I want to point out that the theoretical portion of this work is based largely on a series of lectures he gave while teaching the Electromagnetic Waves (EE 6.30) course during the summer quarter of 1973. His unusual ability to present difficult topics in a way that is easily understood by the student was the largest and most important contribution to the success of this work.

I want to thank Dr. Charles J. Bridgman for his suggestions and helpful comments made during the early stages of the work.

I want to thank Capt Frank N. Fredrickson and Lt John R. Lillis for taking the time to discuss various problems, ideas, and solutions with me.

Last, but not least, I want to gratefully acknowledge the large contribution of my wife, Karen. She offered moral support, punched computer cards, typed drafts, and in many other ways contributed to the successful conclusion of this work.

Terry C. Chapman

Contents

Preface . . . . .	ii
List of Figures . . . . .	iv
Abstract . . . . .	v
I. Introduction . . . . .	1
II. Theory . . . . .	4
Overview . . . . .	4
Electron Current and Densities . . . . .	4
Gamma Transport . . . . .	4
Electron Currents and Densities . . . . .	6
Relativistic Electron Motion . . . . .	9
Transformation to Spherical Coordinates . . . . .	10
Electromagnetic Fields from High Altitude Currents . . . . .	13
Maxwell's Equations . . . . .	13
Transformation to Spherical Coordinates and Retarded Time . . . . .	14
High Frequency Approximation . . . . .	17
III. Code Description . . . . .	20
General Approach . . . . .	20
Inputs . . . . .	24
Preliminary Calculations . . . . .	25
Calculation of Compton Currents and Conductivity . . . . .	25
Integration of Field Equations . . . . .	27
Outputs . . . . .	27
IV. Results of Input Parameter Variation . . . . .	29
V. Discussion and Recommendations . . . . .	40
Limitations . . . . .	40
Uses . . . . .	41
Recommendations . . . . .	41
Bibliography . . . . .	43
Appendix A: EMP Code User's Guide . . . . .	44
Appendix B: EMP Code Flow Charts . . . . .	48
Appendix C: EMP Code Listing . . . . .	57
Vita . . . . .	73

List of Figures

<u>Figure</u>		<u>Page</u>
1.	Geometry of the Burst. . . . .	5
2.	Descriptive Flow Chart . . . . .	21
3.	Target Geometry . . . . .	23
4.	Output from a Typical Run. . . . .	30
5.	Plot of $E(\tau)$ at Target from a Typical Run	31
6.	Variation in the X Direction . . . . .	33
7.	Variation in the Y Direction . . . . .	34
8.	Variation in the Z Direction . . . . .	35
9.	Variation in Height of Burst . . . . .	37
10.	Variation in Gamma Yield . . . . .	39



Abstract

A relatively inexpensive computer code is developed to calculate the peak value of the electric field contained in an electromagnetic pulse generated by the gamma rays from a high altitude nuclear burst. The code is based on the Karzas and Latter theory for the production of Compton electrons and their interaction with the earth's magnetic field.

The code can be used to calculate the peak value of the electric field at a target anywhere on or above ground level, resulting from a nuclear burst above 60 km altitude with a gamma yield up to 60 tons. Either the direct or the ground reflected wave can be calculated. With special care, bursts up to 1 kt of gamma yield can be used.



## A COMPUTER CODE FOR HIGH ALTITUDE EMP

I. Introduction

The effects of a nuclear environment on aerospace systems is an important factor in systems analysis. During the past few years several students have worked with Professor Bridgman at the Air Force Institute of Technology (AFIT) on a computer code to determine survivability of a system with known nuclear vulnerabilities from a variable nuclear threat. The AFIT survivability code capabilities include blast, thermal, x-ray, gamma ray, and neutron effects. The high altitude EMP code presented in this report is intended to be used in conjunction with the AFIT survivability code.

The EMP (electromagnetic pulse) from a nuclear weapon is usually considered to be a radiating electromagnetic wave of short duration containing many frequencies. However, the nuclear generated EMP was not studied seriously until a considerable time after the first nuclear explosion. At present there is a significant amount of work being done to model EMP generation and effects. For example the Air Force Weapons Laboratory (AFWL) and several civilian companies under contract to the USAF are working in the field.

There are several different types of EMP with distinctions made between the mechanisms which generate them. Kinsley (Ref 1) presents a comprehensive discussion of the various types of EMP. For example, a nuclear burst on the ground produces an EMP with different characteristics

than those from a high altitude burst. Also, nuclear burst products interacting directly with a system can produce an EMP within the system or even within the circuits of the system. This report considers only the EMP generated by high altitude burst gamma rays interacting with the atmosphere.

The high altitude EMP code developed in this report is based on the theory of Karzas and Latter (Ref 2). Briefly, the theory develops a model for the interaction of Compton electrons with the geomagnetic field. The Compton electrons are produced by prompt gamma radiation from the burst in a reasonably well defined region in the atmosphere. Several simplifications are made before arriving at the final equations.

Since several of the simplifications and assumptions used are implicit in the presentation of the theory, it is appropriate to list them here. Only one group of monoenergetic unscattered gamma rays are considered to produce Compton electrons. Each gamma which interacts is assumed to produce one and only one Compton electron initially traveling precisely in the radial direction. No angular distribution of Compton electrons is allowed. All Compton electrons are assumed to have the same energy. Curvature of the Earth's magnetic field is ignored. The electromagnetic fields are not self-consistent, that is, only the geomagnetic field is considered to affect the motion of the Compton electrons. Cascading of secondary electrons and recombination of ions is ignored. The low

frequency portion of the pulse is not considered. The Earth is assumed to be flat and the finite conductivity of ground is not considered. The burst is assumed to be far from the absorption region. Only gamma ray effects are considered.

Although the final model is somewhat restricted by these assumptions and simplifications, the end result is a relatively inexpensive computer code which gives a peak value of the electric field at any target point on or above the ground, which is an upper bound on the actual peak value.

Section II of this report develops the theory and derives the equations used in the code. Section III describes the calculational procedures used in the code. Section IV presents a sample of typical results and a study of input parameter variation. Section V is a discussion of the code's limitations and uses, with recommendations for possible improvements. Appendix A is a code user's guide. Appendix B is the detailed flow charts for the entire code. And finally Appendix C is a listing of the complete code.

## II. Theory

### Overview

The EMP problem is a problem in classic electromagnetic theory. A solution of Maxwell's equations is a solution of the problem. In this case it is necessary to model the current and charge densities generated by the gamma rays in the absorption region to obtain the sources and conductivity needed to solve Maxwell's equations.

Expressions for the current sources and conductivity are obtained in four steps. The transport of the gammas from the burst to the absorption region is used to obtain the number density of reacting gammas. This result is used with the models for the current and charge densities to obtain preliminary expressions. Then after considering the relativistic motion of the Compton electrons, the preliminary expressions are transformed to spherical coordinates.

After presenting Maxwell's equations in a convenient form, they are transformed to spherical coordinates and retarded time. A high frequency approximation is then made to arrive at the final equations.

### Electron Current and Density

Gamma Transport. Consider the geometry shown in Fig. 1. The nuclear burst occurs at the origin at time,  $t = 0$ . The gamma rays move to point  $r'$  in time  $t'$  and at that point and time interact to create Compton electrons. It is assumed

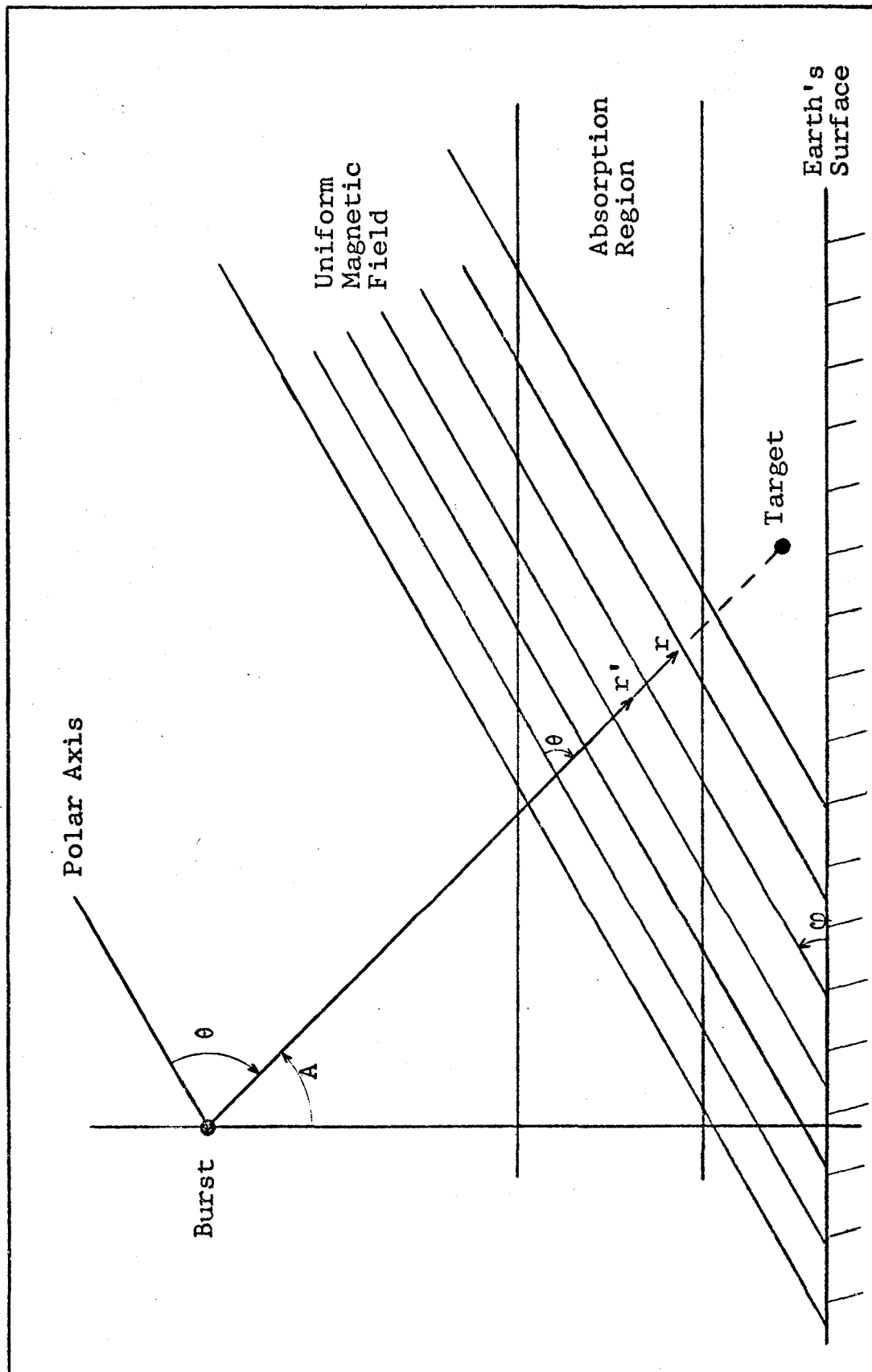


Fig. 1. Geometry of the Burst

that each gamma creates one and only one Compton electron traveling in the radial direction with the maximum Compton recoil energy.

The gamma ray emission rate can be taken as

$$\frac{dN(t)}{dt} = \frac{Y}{E} f(t) \quad (1)$$

where

$N(t)$  = number of gamma rays emitted

$Y$  = gamma ray yield of burst

$E$  = mean energy of the gamma rays

$f(t)$  = time dependence of the yield

and

$$\int_{-\infty}^{\infty} f(t) dt = 1 \quad (2)$$

The number density of gammas,  $g(r)$ , which interact at a point,  $r$ , can be taken as

$$g(r) = \frac{Y}{E} \frac{\exp \left\{ -\int_0^r \frac{dr'}{\lambda(r')} \right\}}{4\pi r^2 \lambda(r)} \quad (3)$$

where

$\lambda$  = mean free path for production of Compton electrons.

Electron Currents and Densities. The rate of production of primary (Compton) electron density,  $n_{\text{pri}}$ , is

$$\frac{dn_{\text{pri}}}{dt} = g(r) f(t - r/c) \quad (4)$$



Following the Karzas-Latter approach (Ref 2) it is assumed that the electrons maintain their initial speed,  $V_0$ , throughout their range,  $R$ , and then abruptly stop. Also, it is assumed that the secondary electrons are made at a uniform rate during the lifetime,  $R/V_0$ , of the Compton electrons. Therefore, the rate of production of secondary electron density,  $n_{\text{sec}}$ , is

$$\frac{dn_{\text{sec}}}{dt} = \left\{ \frac{E_{\text{pri}}/33\text{ev}}{R/V_0} \right\} n_{\text{pri}} = \frac{qV_0}{R} n_{\text{pri}} \quad (5)$$

where

$E_{\text{pri}}$  = the initial energy of the Compton electrons

$R$  = the range of the Compton electrons in air

$q$  =  $E_{\text{pri}}/33\text{ev}$

$33\text{ev}$  = average ionization energy per molecule for air

$V_0$  = the speed of the Compton electrons

$R/V_0$  = the lifetime of the Compton electrons

Now consider the current resulting from the Compton electrons. The differential current is the charge times the velocity times the differential density of electrons. Hence

$$d\vec{J}^c = -e\vec{V}(t-t')g(r')f(t' - r'/c)dt' \quad (6)$$

where

$\vec{V}(t-t')$  = velocity of the Compton electrons at  
time  $t$  which were created at time  $t'$ .

Putting (6) into integral form gives

$$\vec{J}^c = -e \int_{t-R/V_0}^t g(r') f(t' - r'/c) \vec{V}(t-t') dt' \quad (7)$$

Now let

$$\tau' = t - t' \quad (8a)$$

$$\tau = t - (r/c) \quad (8b)$$

$$X(\tau') = X(\tau) = r - r' \quad (8c)$$

Also note that

$$(r-r') \ll r \text{ or } r' \quad (9)$$

for distant explosions (see Fig. 1). So,

$$g(r) \approx g(r') \quad (10)$$

Using Eqs (8), (9), and (10) in Eq (7) gives

$$\vec{J}^c = -eg(r) \int_0^{R/V_0} \vec{V}(\tau') f\left(\tau - \tau' + \frac{X(\tau')}{c}\right) d\tau' \quad (11)$$

Using similar arguments,

$$n_{\text{pri}} = g(r) \int_0^{R/V_0} f\left(\tau - \tau' + \frac{X(\tau')}{c}\right) d\tau' \quad (12)$$

And putting Eq (12) into Eq (5) yields

$$\begin{aligned}
 n_{\text{sec}} &= \frac{qV_0}{R} \int_{-\infty}^{\tau} n_{\text{pri}}(\tau') d\tau' \\
 &= g(\tau) \frac{qV_0}{R} \int_{-\infty}^{\tau} \left[ \int_0^{R/V_0} f\left(\tau' - \tau'' + \frac{X(\tau'')}{c}\right) d\tau'' \right] d\tau' \quad (13)
 \end{aligned}$$

Relativistic Electron Motion. Equations (11), (12), and (13) contain  $r(\tau)$  and  $X(\tau)$  which are not yet defined in an easily obtained form. The equation of motion for a Compton electron is

$$\frac{d}{dt} (m\gamma \vec{V}) = -e\vec{V} \times \vec{B}_0 \quad (14)$$

where

$m$  = electron rest mass

$\gamma = [1 - (V/c)^2]^{-1/2}$

$\vec{B}_0$  = earth's magnetic field =  $B_0 \hat{U}_z$

Again it is assumed that  $V_0$  is constant throughout the electron's lifetime.

With  $\omega = eB_0/m\gamma$  Eq (14) becomes

$$\frac{d}{d\tau} \vec{V}(\tau) = -\vec{V}(\tau) \times \hat{U}_z \omega \quad (15)$$

Breaking Eq (15) into its rectangular components

$$\frac{dV_x}{d\tau} = -\omega V_y \quad (16a)$$

$$\frac{dV_y}{d\tau} = \omega V_x \quad (16b)$$

$$\frac{dV_z}{d\tau} = 0 \quad (16c)$$

A solution for this set of equations is

$$V_x = V_{\perp} \cos \omega\tau \quad (17a)$$

$$V_y = V_{\perp} \sin \omega\tau \quad (17b)$$

$$V_z = V_{\parallel} \quad (17c)$$

where  $V_{\perp}$  is the initial velocity component perpendicular to  $\vec{B}_0$  and  $V_{\parallel}$  is the initial velocity component parallel to  $\vec{B}_0$  and both are constants with respect to  $\tau$ .

Transformation to Spherical Coordinates. It is convenient to transform the above solution to a spherical coordinate system with its origin at the burst point. The transformation from rectangular to spherical coordinates is

$$V_r = V_x \sin \theta \cos \phi + V_y \sin \theta \sin \phi + V_z \cos \theta \quad (18a)$$

$$V_{\theta} = V_x \cos \theta \cos \phi + V_y \cos \theta \sin \phi - V_z \sin \theta \quad (18b)$$

$$V_{\phi} = -V_x \sin \phi + V_y \cos \phi \quad (18c)$$

Without loss of generality the coordinates can be chosen such that  $\vec{V}$  lies in the X-Y plane, hence  $\theta = 90^\circ$ , and the transformation becomes

$$V_r = V_x \sin \theta + V_z \cos \theta \quad (19a)$$

$$V_\theta = V_x \cos \theta - V_z \sin \theta \quad (19b)$$

$$V_\phi = V_y \quad (19c)$$

Note that

$$V_\perp = V_0 \sin \theta \quad (20a)$$

$$V_\parallel = V_0 \cos \theta \quad (20b)$$

Putting Eqs (17) and (20) into Eq (19) gives

$$V_r = V_0 [\sin^2 \theta \cos \omega \tau + \cos^2 \theta] \quad (21a)$$

$$V_\theta = V_0 [\cos \theta \sin \theta \cos \omega \tau - \sin \theta \cos \theta] \quad (21b)$$

$$V_\phi = V_0 [\sin \theta \sin \omega \tau] \quad (21c)$$

Now  $X(\tau)$  can be written as

$$X(\tau) = \int_0^\tau V_r d\tau = V_0 [\sin^2 \theta \frac{\sin \omega \tau}{\omega} + \tau \cos^2 \theta] \quad (22)$$

Equations (21) and (22) substituted into Eq (11) give

$$J_r^c = -eg(r)V_0 \int_0^{R/V_0} f(T) [\cos^2 \theta + \sin^2 \theta \cos \omega \tau'] d\tau' \quad (23)$$

$$J_\theta^c = -eg(r)V_0 \int_0^{R/V_0} f(T) [\sin \theta \cos \theta (\cos \omega \tau' - 1)] d\tau' \quad (24)$$

$$J_\phi^c = -eg(r)V_0 \int_0^{R/V_0} f(T) [\sin \theta \sin \omega \tau'] d\tau' \quad (25)$$

where

$$T = \tau - (1 - \beta \cos^2 \theta) \tau' + \beta \sin^2 \theta \frac{\sin \omega \tau'}{\omega} \quad (26a)$$

with

$$\beta = v_0/c \quad (26b)$$

Equations (23), (24), (25), and (26) provide the Compton currents within the absorption region in a form which can be used in the final field equations. In addition to the Compton currents, an expression for the conductivity within the absorption region is needed.

Equations (21) and (22) substituted into Eq (13) give

$$n_{sec}(\tau) = \frac{qV_0}{R} g(r) \int_{-\infty}^{\tau} \left[ \int_0^{R/V_0} f(T') d\tau'' \right] d\tau' \quad (27)$$

where

$$T' = \tau' - (1 - \beta \cos^2 \theta) \tau'' + \beta \sin^2 \theta \frac{\sin \omega \tau''}{\omega} \quad (28)$$

Consider the equation of motion for secondary electrons. Neglecting the  $\vec{V} \times \vec{B}_0$  term, which is small compared to the other terms (Ref 2) it is

$$m \frac{d\vec{V}}{dt} = -e\vec{E} - m\vec{V}v_c \quad (29)$$

where

$v_c$  = electron collision frequency.

These secondary electrons have velocities in the thermal region and are assumed to reach their maximum velocity instantly. In this case, Eq (29) becomes

$$\vec{V} = \frac{-e}{mv_c} \vec{E} \quad (30)$$

The current source from the secondary electrons is

$$\vec{J}^{sec} = -e\vec{V}(\tau)n_{sec}(\tau) = \frac{n_{sec}(\tau)}{mv_c} e^2 \vec{E} \quad (31)$$

or in terms of conductivity

$$\vec{J}^{sec} = \sigma(\tau)\vec{E} \quad (32)$$

where

$$\sigma(\tau) = \frac{n_{sec}(\tau)}{mv_c} e^2 \quad (33)$$

Equations (32) and (33) provide the needed expressions for the conductivity.

### Electromagnetic Fields from High Altitude Currents

Maxwell's Equations. Now that the Compton currents and the conductivity due to secondary electrons have been obtained, consider the field equations.

Maxwell's equations are

$$\vec{\nabla} \times \vec{E} = - \frac{\partial \vec{B}}{\partial t} \quad (34a)$$

$$\vec{\nabla} \times \vec{B} = \mu_0 \vec{J} + \frac{1}{c^2} \frac{\partial \vec{E}}{\partial t} \quad (34b)$$

$$\vec{\nabla} \cdot \vec{E} = \frac{q_v}{\epsilon_0} \quad (34c)$$

$$\vec{\nabla} \cdot \vec{B} = 0 \quad (34d)$$

where

$\vec{J}$  = total current density

$q_v$  = total charge density

Continuity of charge requires

$$\frac{\partial q_v}{\partial t} + \vec{\nabla} \cdot \vec{J} = 0 \quad (35)$$

It is convenient to combine the above equations into equations containing only  $\vec{E}$  in one and only  $\vec{B}$  in the other. Doing so gives

$$\left( \nabla^2 - \frac{1}{c^2} \frac{\partial^2}{\partial t^2} \right) \vec{E} = \mu_0 \frac{\partial \vec{J}}{\partial t} + \frac{1}{\epsilon_0} \vec{\nabla} q_v \quad (36)$$

$$\left( \nabla^2 - \frac{1}{c^2} \frac{\partial^2}{\partial t^2} \right) \vec{B} = -\mu_0 \vec{\nabla} \times \vec{J} \quad (37)$$

Transformation to Spherical Coordinates and Retarded Time. Equations (36) and (37) will now be transformed to spherical coordinates and retarded time. Consider the transformation



$$\tau = t - r/c \quad (38a)$$

$$r' = r \quad (38b)$$

$$\theta' = \theta \quad (38c)$$

$$\phi' = \phi \quad (38d)$$

This is a spherical coordinate system where time is measured at each radial point in terms of the arrival of the bomb gamma rays at that point.

Using Eq (38) it is easily shown that

$$\frac{\partial}{\partial t} = \frac{\partial}{\partial \tau} \quad (39)$$

$$\frac{\partial}{\partial r} = \frac{\partial}{\partial r'} - \frac{1}{c} \frac{\partial}{\partial \tau} \quad (40)$$

$$\frac{\partial}{\partial \theta} = \frac{\partial}{\partial \theta'} \quad (41)$$

$$\frac{\partial}{\partial \phi} = \frac{\partial}{\partial \phi'} \quad (42)$$

Thus the operator

$$\frac{\partial}{\partial t}$$

transforms to

$$\frac{\partial}{\partial \tau}$$

and the operator

$$\vec{\nabla}$$

transforms to

$$\vec{\nabla} = \hat{U}_r \frac{1}{c} \frac{\partial}{\partial \tau}$$

Similarly, the operator

$$\nabla^2 = \frac{1}{c^2} \frac{\partial^2}{\partial t^2}$$

transforms to

$$\nabla^2 = \frac{2}{c} \frac{\partial}{\partial \tau} \frac{1}{r} \frac{\partial}{\partial r} r$$

Equation (36) now becomes

$$\left[ \nabla^2 - \frac{2}{c} \frac{1}{r} \frac{\partial}{\partial \tau} \frac{\partial}{\partial r} r \right] \vec{E} = \mu_0 \frac{\partial \vec{J}}{\partial \tau} + \frac{1}{\epsilon_0} \vec{\nabla} q_v - \hat{U}_r \frac{1}{c} \frac{\partial q_v}{\partial \tau} \quad (43)$$

and Eq (35) becomes

$$\frac{\partial q_v}{\partial \tau} = -\vec{\nabla} \cdot \vec{J} + \hat{U}_r \frac{1}{c} \frac{\partial}{\partial \tau} \cdot \vec{J} = -\vec{\nabla} \cdot \vec{J} + \frac{1}{c} \frac{\partial J_r}{\partial \tau} \quad (44)$$

Using Eq (44) in Eq (43) and rearranging gives

$$\begin{aligned} & -\nabla^2 \vec{E} + \hat{U}_r \frac{1}{c \epsilon_0} \vec{\nabla} \cdot \vec{J} + \frac{1}{\epsilon_0} \vec{\nabla} q_v \\ & + \frac{\partial}{\partial \tau} \left[ \frac{2}{c} \frac{1}{r} \frac{\partial}{\partial \tau} (r \vec{E}) + \mu_0 (\vec{J} - \hat{U}_r J_r) \right] = 0 \end{aligned} \quad (45)$$

Similarly, Eq (37) becomes

$$\begin{aligned}
 & -\nabla^2 \vec{B} + \mu_0 \vec{\nabla} \times \vec{J} + \frac{\partial}{\partial \tau} \left[ \frac{2}{rc} \frac{\partial}{\partial r} (r \vec{B}) \right] \\
 & + \frac{\partial}{\partial \tau} \left[ \frac{\mu_0}{c} (\hat{U}_\phi J_\phi - \hat{U}_\theta J_\theta) \right] = 0
 \end{aligned} \tag{46}$$

High Frequency Approximation. Again, following the Karzas-Latter model, note that the variation of currents with distance is slow compared to variations with time and that the fields resulting from the transverse currents are rapidly varying in character, as are the currents themselves. Therefore, only the  $\partial/\partial \tau$  terms are kept in the transverse field equations. Since the radial components do not propagate outside of the absorption region, they are not considered further in this report.

The transverse equations become

$$\frac{\partial}{\partial \tau} \left[ \frac{2}{c} \frac{1}{r} \frac{\partial}{\partial r} (r E_\theta) + \mu_0 J_\theta \right] = 0 \tag{47}$$

$$\frac{\partial}{\partial \tau} \left[ \frac{2}{c} \frac{1}{r} \frac{\partial}{\partial r} (r E_\phi) + \mu_0 J_\phi \right] = 0 \tag{48}$$

$$\frac{\partial}{\partial \tau} \left[ \frac{2}{c} \frac{1}{r} \frac{\partial}{\partial r} (r B_\theta) - \frac{\mu_0}{c} J_\phi \right] = 0 \tag{49}$$

$$\frac{\partial}{\partial \tau} \left[ \frac{2}{c} \frac{1}{r} \frac{\partial}{\partial r} (r B_\phi) + \frac{\mu_0}{c} J_\theta \right] = 0 \tag{50}$$

These equations are called the Karzas-Latter high frequency approximation for the EMP fields, and they are useful in the range  $0 < \tau < 100$  shakes.

Integration with respect to time yields

$$\frac{2}{c} \frac{1}{r} \frac{\partial}{\partial r} (rE_{\theta}) + \mu_0 J_{\theta} = 0 \quad (51)$$

$$\frac{2}{c} \frac{1}{r} \frac{\partial}{\partial r} (rE_{\phi}) + \mu_0 J_{\phi} = 0$$

$$\frac{2}{c} \frac{1}{r} \frac{\partial}{\partial r} (rB_{\theta}) - \frac{\mu_0}{c} J_{\phi} = 0 \quad (53)$$

$$\frac{2}{c} \frac{1}{r} \frac{\partial}{\partial r} (rB_{\phi}) + \frac{\mu_0}{c} J_{\theta} = 0 \quad (54)$$

Recall that the total current density is

$$\vec{J} = \vec{J}^{\text{pri}} + \vec{J}^{\text{sec}} = \vec{J}^c + \sigma(\tau)\vec{E} \quad (55)$$

so Eqs (51) and (52) become

$$\frac{2}{c} \frac{1}{r} \frac{\partial}{\partial r} (rE_{\theta}) + \mu_0 J_{\theta}^c + \mu_0 \sigma(\tau) E_{\theta} = 0 \quad (56)$$

$$\frac{2}{c} \frac{1}{r} \frac{\partial}{\partial r} (rE_{\phi}) + \mu_0 J_{\phi}^c + \mu_0 \sigma(\tau) E_{\phi} = 0 \quad (57)$$

With the aid of a computer, it is now possible to obtain numerical solutions for the above equations which will yield a slightly high estimate of the peak value of the EMP pulse resulting from a high altitude burst.

Below the absorption region the Compton currents and the conductivity are zero. In this case, Eqs (56) and (57) have the following solutions:

$$E_{\theta} = C_1/r \quad (58)$$

$$E_{\phi} = C_2/r \quad (59)$$

where  $C_1$  and  $C_2$  are determined by the values of  $E_{\theta}$ ,  $E_{\phi}$ , and  $r$  at the bottom of the absorption region.

### III. Code Description

#### General Approach

Equations (56), (57), (58), and (59) were chosen as the simplest ones to solve numerically. Of course, Eqs (24), (25), (27), and (33) are used to obtain the Compton currents and conductivity needed to solve Eqs (56) and (57).

The B - field equations are not solved since

$$E = cB \quad (60)$$

can be used to obtain B once E is found. This relationship is based on the assumption that the EMP pulse is a spherical wave propagating in free space, below the absorption region.

The function used for the time dependence of the weapon yield is the one recommended by Pomranning (Ref 3).

$$f(\tau) = (1/N) \frac{(\alpha+\beta) \exp(\tau-\tau_0)}{\beta + \alpha \exp[(\alpha+\beta)(\tau-\tau_0)]} \quad (61)$$

where N is chosen such that

$$\int_0^{\infty} f(\tau) d\tau = 1 \quad (62)$$

and  $\alpha > \beta$ .

This function rises like  $e^{\alpha\tau}$  for small  $\tau$ , falls like  $e^{-\beta\tau}$  for large  $\tau$ , and has a single maximum at  $\tau_0$ .

Figure 2 presents a flow chart which is descriptive of the approach taken solving the equations. The top of the absorption region is assumed to be at 50 km altitude and the bottom of the absorption region is assumed to be

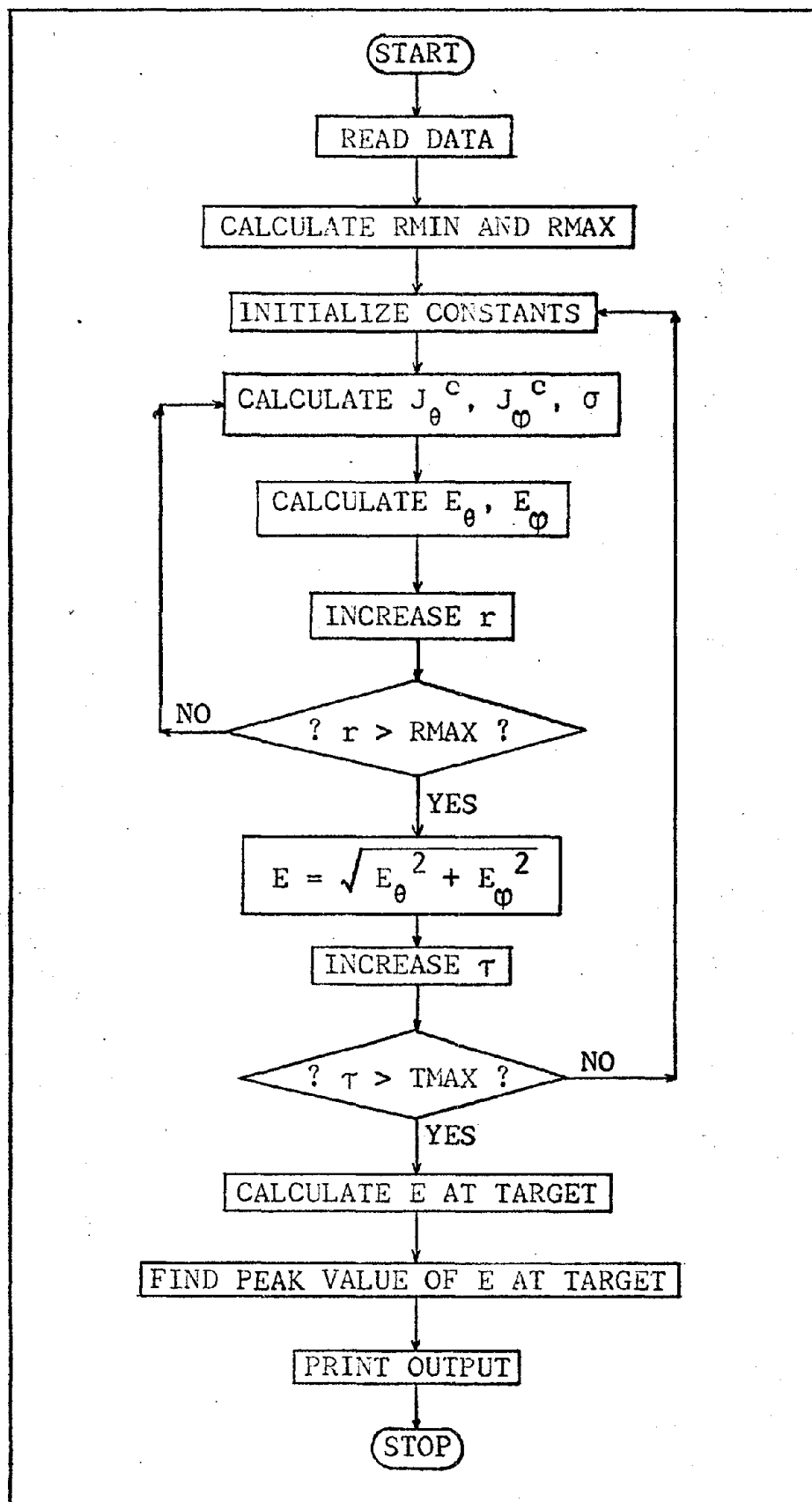


Fig. 2. Descriptive Flow Chart

at 20 km altitude. Calculations by Latter and LeLevier (Ref 4) indicate that 20 km to 50 km is the altitude where most of the prompt gamma ray energy is deposited.

Figure 3 depicts the target geometry. The value for  $R_{MIN}$  is determined by the intersection of the line of sight with the 50 km altitude. The value for  $R_{MAX}$  is determined by the intersection of the line of sight with the 20 km altitude. If the target is in the absorption region the target altitude determines  $R_{MAX}$  for the direct wave calculation. These two values of  $r$  are the limits on the mesh in the  $r$  direction. The line of sight is divided into the desired number of steps along  $r$  for the integration on  $r$  in the absorption region.

The retarded time direction of the mesh is divided into 0.1 shake steps up to 10 shakes and then 1.0 shake steps on up to 100 shakes. Calculation can be stopped at any desired  $T_{MAX}$  from 10 to 100 shakes, which is the upper limit of the usefulness of the high frequency approximation.

If the ground reflected wave is to be calculated, the mirror image of the target, below ground, is used to find the line of sight from the burst to the target. (Refer to Fig. 3.)

At  $r = R_{MIN}$  all of the fields are assumed to be zero. For each  $\tau$ , equations (57) and (58) are integrated over  $r$  from  $R_{MIN}$  to  $R_{MAX}$  and the value of  $E$  at the bottom of the absorption region is stored. At each step in  $r$ , equations (24), (25), and (27) are numerically integrated. Then



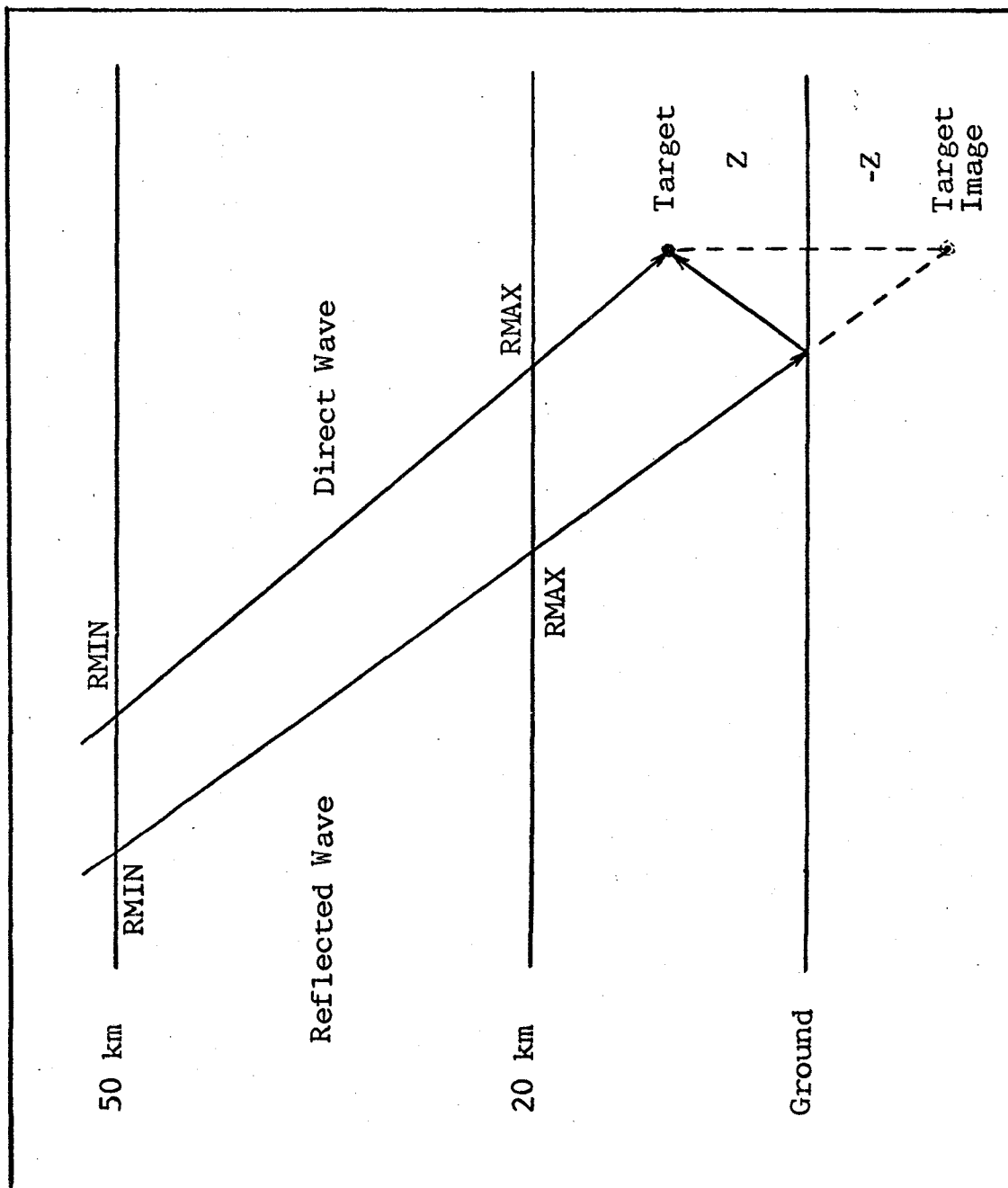


Fig. 3. Target Geometry

equations (58) and (59) are combined into

$$E = \frac{(R_{MAX})(E_{R_{MAX}})}{r_{target}} \quad (63)$$

to find E at the target.

The E array is then searched to find the peak value before printing out the results.

### Inputs

The code uses a right handed Cartesian coordinate system with the ground in the X-Y plane, the  $\vec{B}_0$  vector in the Y-Z plane, and  $\hat{j}$  pointing towards the equator. For example, in the northern hemisphere,  $\hat{i}$  is magnetic west,  $\hat{j}$  is magnetic south, and  $\hat{k}$  is altitude. The origin of the coordinate system is always at ground zero, directly below the burst. Note that this coordinate system is not the same as the Cartesian systems used earlier.

Referring to the above coordinate system the target coordinates, (X,Y,Z), are read in using units of meters. If the reflected wave is to be calculated the altitude is read in as a negative number, (X,Y,-Z).

The height of the burst is read in using units of kilometers. The gamma yield of the burst is read in using units of kilotons.

The magnitude of the Earth's magnetic field is read in using units of webers per square meter. The dip angle ( $\phi$  in Fig. 1) of the magnetic field is read in using units of degrees.

NDELR, the desired number of steps to be used in the integration over  $r$  in the absorption region, is read in as any integer in the closed interval  $[50, 500]$ .

TMAX, the retarded time where calculations are to be stopped, is read in, using units of shakes, as any integer in the closed interval  $[10, 100]$ .

### Preliminary Calculations

Before starting the numerical integrations, the code performs several preliminary calculations. The input data is converted to MKS units. The reflected wave is used whenever  $Z$  is greater than 49 km or less than 0. The target coordinates are transformed to a spherical coordinate system with the burst at the origin and the polar axis parallel to  $\vec{B}_0$ . The line of sight intersections with the absorption region are determined. And finally, the constant angles required by the code,  $\theta$  and  $A$ , (see Fig. 1) are calculated.

### Calculation of Compton Currents and Conductivity

The two Compton currents,  $J_\theta^C$  and  $J_\phi^C$  are calculated at each  $r, \tau$  mesh point by numerically integrating equations (24) and (25). The step size used is 0.1 times the Compton lifetime,  $R/V_0$ . The integration itself is done using the 4<sup>th</sup> order Runge-Kutta method (Ref 5). It should be noted that both the mean free path for Compton interaction and the Compton lifetime are exponentially scaled from sea

level values using a 7 km scale height. However, the Compton lifetime is not allowed to be greater than 100 shakes, since this is the maximum time of interest.

Monoenergetic gammas of energy 1.5 Mev are assumed. The most energetic Compton electrons resulting from 1.5 Mev gammas have a speed of  $2.88 (10)^8$  m/sec. Therefore  $V_0 = 2.88 (10)^8$  m/sec.

Since the integration on  $\tau''$  in equation (27) is also over the Compton lifetime, this integration is carried out simultaneously with the Compton current integrations. Again, the 4<sup>th</sup> order Runge-Kutta method is used. It is broken into two parts, one for  $-\infty < \tau' < 0$  and the other for  $0 < \tau' < \tau$ . In this case,  $-\infty$  is defined to be the time when the first gamma ray reached the top of the absorption region, since no secondaries can be produced before that time.

The integration on  $\tau'$  in equations (27) is also broken into two parts, one for  $-\infty < \tau' < 0$  and the other for  $0 < \tau' < \tau$ . In the first case, integration is started at  $\tau' = 0$  and proceeds to  $\tau' = -(r-R_{MIN})/V_0$  in steps of  $\Delta\tau' = -\Delta r/V_0$ . In the second case, integration is started at  $\tau' = 0$  and proceeds to  $\tau' = \tau$  in steps of  $\Delta\tau' = \Delta\tau$ . In both cases, simple step integration is used. That is

$$\int f(\tau') d\tau' = \sum_{\text{all } i} (\Delta\tau'_i) [f(\tau'_i)] \quad (64)$$

The integration over  $\tau'$  is carried out parallel to the integration of (56) and (57) over  $r$  (using space as a pseudo retarded time) and simultaneously with the increase in  $\tau$  as the space integrations are repeated for each new  $\tau$ .

This rather involved approach to solving equation (27) is necessary to save running time. A direct approach, with separate integrations, would at least triple or quadruple the total running time required for execution of the code.

### Integration of the Field Equations

For each  $\tau$ , equations (56) and (57) are integrated from  $r = RMIN$  to  $r = RMAX$  in steps of  $\Delta r = (RMAX - RMIN)/NDEL R$  using the 4<sup>th</sup> order Runge-Kutta method. Then the magnitude of  $E$  is found from the two components and the result is stored in the  $E$  array.  $\tau$  is increased by  $\Delta\tau$  and the whole process is repeated until  $\tau$  reaches  $TMAX$ .

On completion of the iterations, each member of the  $E$  array is multiplied by  $RMAX/r_{target}$  (equation 62). Then the  $E$  array is searched to find the peak value.

### Outputs

There are several output options available in the code. The basic output is:

1. Gamma yield and altitude of burst.
2. Target coordinates from ground zero.
3. Distance from burst to target.
4. A message indicating whether the direct or the reflected wave is being calculated.

5. The time period covered by the calculation.
6. The time when the peak value occurred.
7. The peak value of  $E$  at the target.
8. The  $\tau$  and  $E$  arrays.

In addition, a linear and a log-log plot of  $E(\tau)$  can be obtained. Also, a listing of the values of  $E$  at the bottom of the absorption region for each  $\tau$  can be obtained. Either or both of these two options can be added to the basic output.

#### IV. Results and Input Parameter Variation

The output from a typical run is shown in Fig. 4.

The  $E(\tau)$  calculated during the run is shown in Fig. 5.

The input data for this run was:

X = 0 meters (65a)

Y = 0 meters (65b)

Z = 0 meters (65c)

HOB = 100 km (65d)

$Y_Y$  = .001 kt (65e)

$B_0$  =  $2(10)^{-5}$  wb/m<sup>2</sup> (65f)

Dip Angle = 20° (65g)

NDEL R = 50 (65h)

TMAX = 20 shakes (65i)

The CDC 6600 Computer required 191 sec and 33000<sub>8</sub> words of central memory to execute this run.

The peak value of E, 6400 V/m, obtained in this run compares favorably with Karzas-Latter's order of magnitude estimate of  $10^4$  V/m (Ref 2) from similar input data.

In order to gain a better knowledge of the operating capabilities of the code, the effect of varying input parameters one at a time was studied. The basic set of parameters used was:

THE BURST WITH GAMMA YIELD CF 1.000E-03 KILOTCNS  
IS AT AN ALTIITUDE OF 1.000E+02 KILOMETERS.

THE TARGET IS AT CCORCINATES 0. 0.  
WHICH IS 1.000E+05 METERS FROM THE BURST

DIRECT WAVE IS BEING CALCULATED

ITERATION TERMINATED AFTER 20.0 SHAKES

PEAK OCCURRED AT 2.1 SHAKES

\* \* \* \* \*  
\* PEAK EFIELD AT TARGET IS 6.448E+03 VOLTS/METER \*  
\* \* \* \* \*

Fig. 4. Output from a Typical Run



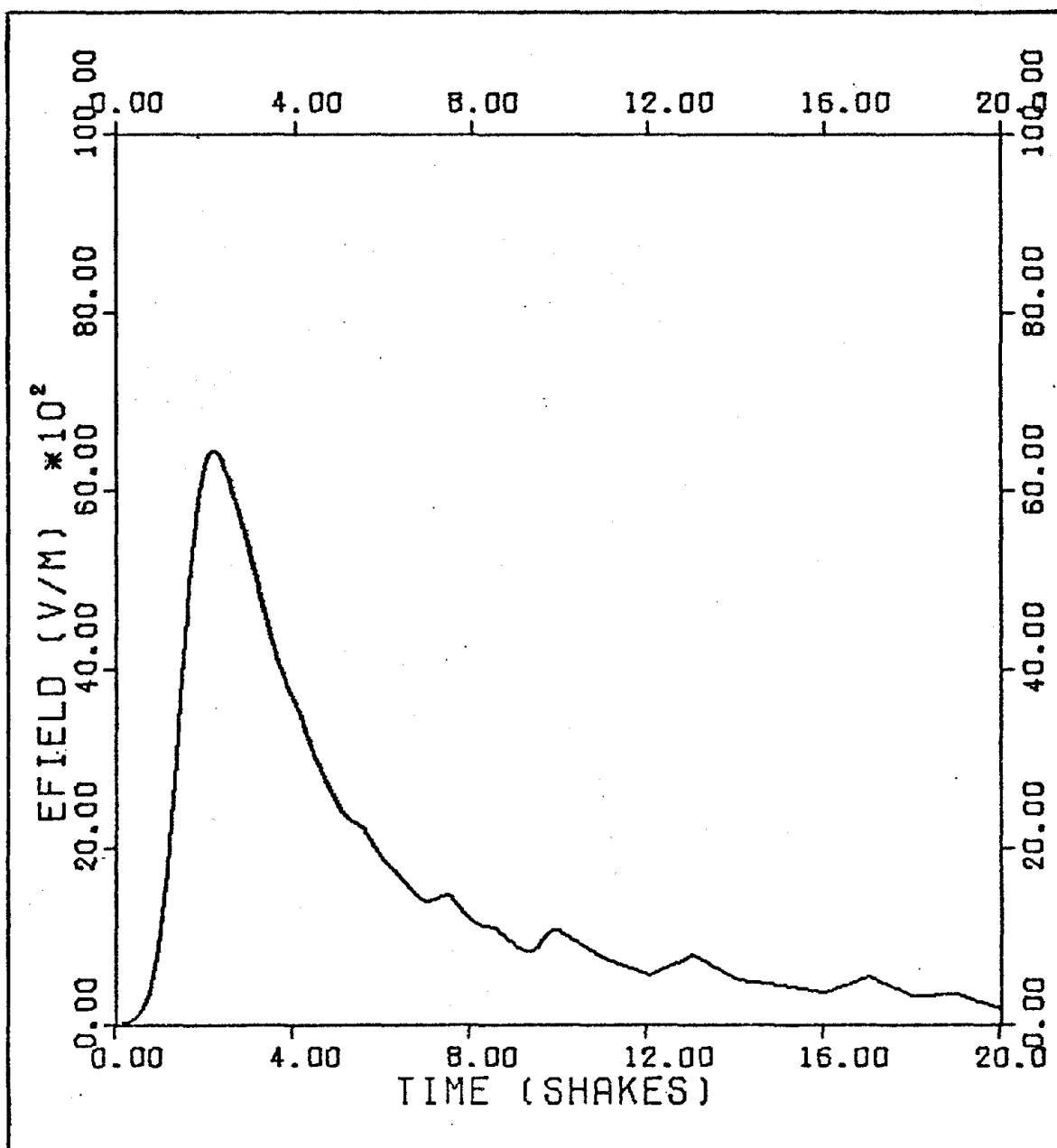


Fig. 5. Plot of  $E(\tau)$  at target from a typical run

$$X = 0 \text{ meters} \quad (66a)$$

$$Y = 0 \text{ meters} \quad (66b)$$

$$Z = 0 \text{ meters} \quad (66c)$$

$$HOB = 100 \text{ km} \quad (66d)$$

$$Y_Y = .001 \text{ kt} \quad (66e)$$

Each of the above parameters was systematically varied while holding the others constant. The other inputs were held constant at the values shown in equations (65).

The results of the variation in X are shown in Fig. 6. Since the X axis is perpendicular to the magnetic field the symmetry about  $X = 0$  is expected. The decrease in peak value of E for increasing distance from ground zero is due to the increasing distance from the burst.

The results of the variation in Y are shown in Fig. 7. Here the peak values of E depend on the angle between  $\vec{r}$  and  $\vec{B}_0$ ,  $\theta$ . When  $\theta = 180^\circ$  ( $A = -70^\circ$  and  $Y = -275 \text{ km}$ ) the peak E drops to zero. The maximum peak E is skewed toward  $A = 20^\circ$  ( $\theta = 90^\circ$  and  $Y = 36 \text{ km}$ ). The maximum is not exactly at  $A = 20^\circ$  because of the increased distance from the burst. These characteristics are expected since an electron moving perpendicular to the magnetic field would feel the strongest acceleration from it while an electron moving parallel to the magnetic field would feel no acceleration at all.

The results of variation in Z are shown in Fig. 8. In this case, both the direct and the reflected waves were calculated at each point below the top of the absorption

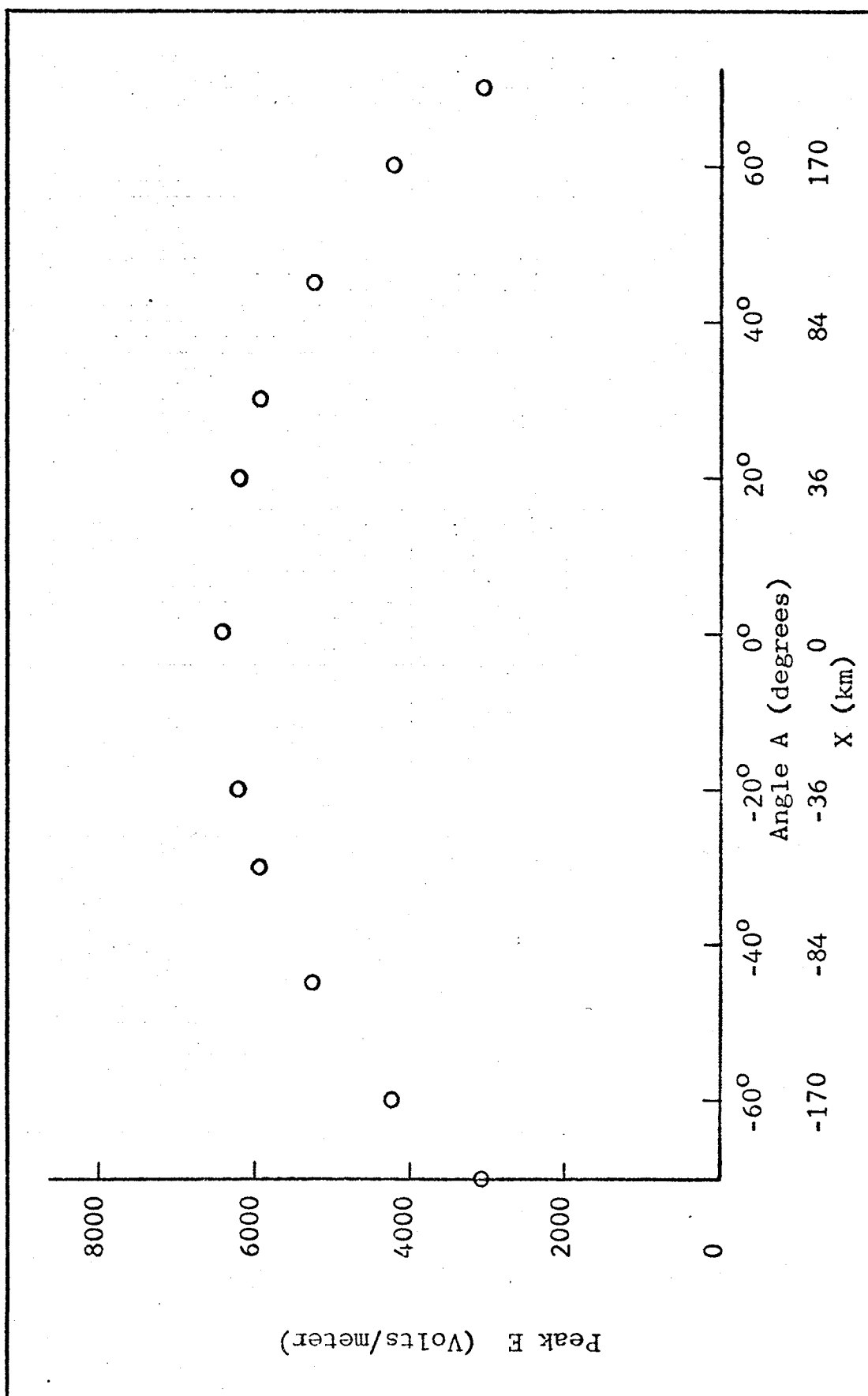


Fig. 6. Variation in the X Direction ( $Y=0$ ,  $Z=0$ ,  $HOB=100\text{km}$ ,  $Y_Y=0.001\text{kt}$ )

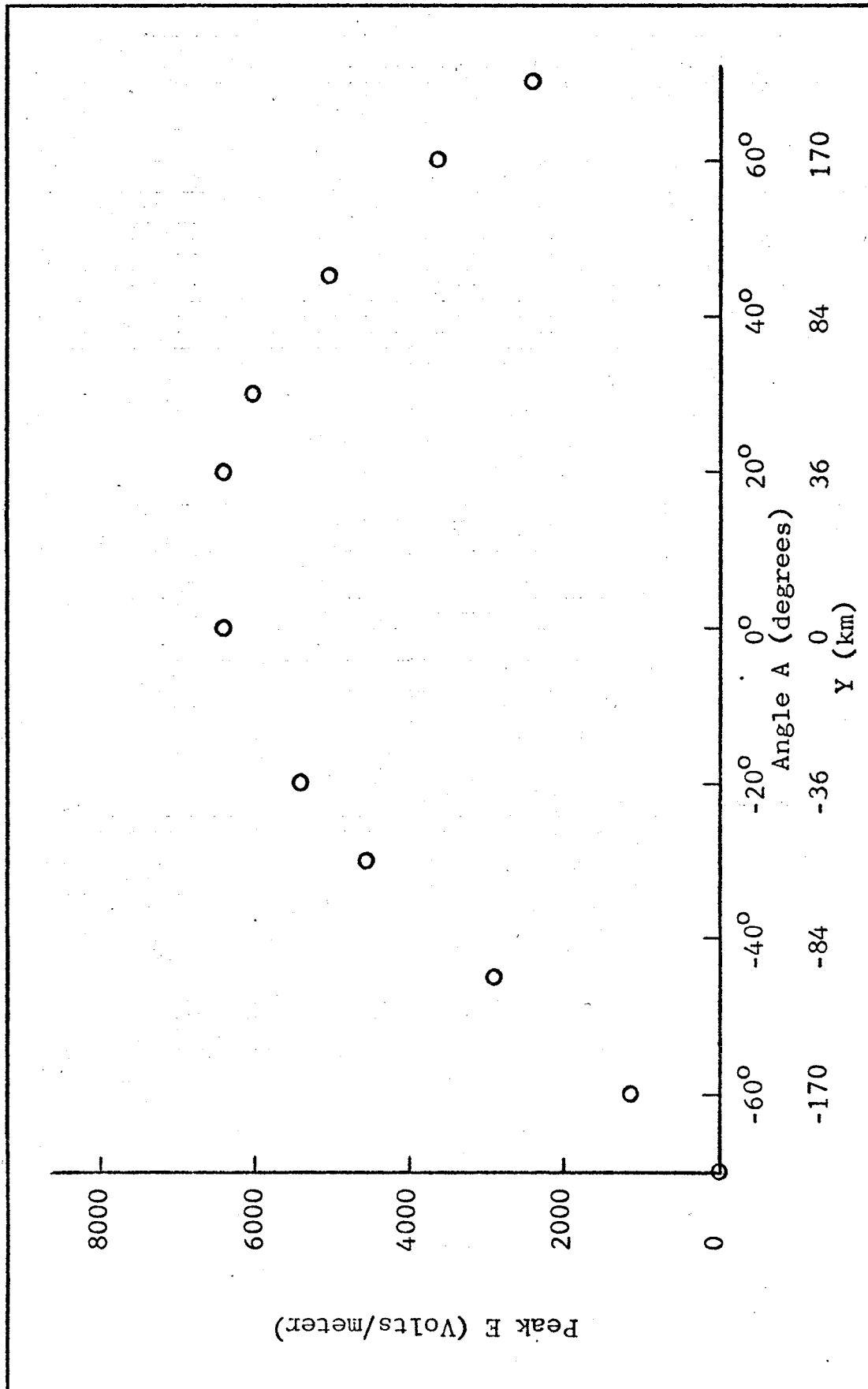


Fig. 7. Variation in Y direction ( $X=0$ ,  $Z=0$ ,  $HOB=100\text{km}$ ,  $Y_Y=.001\text{kt}$ )

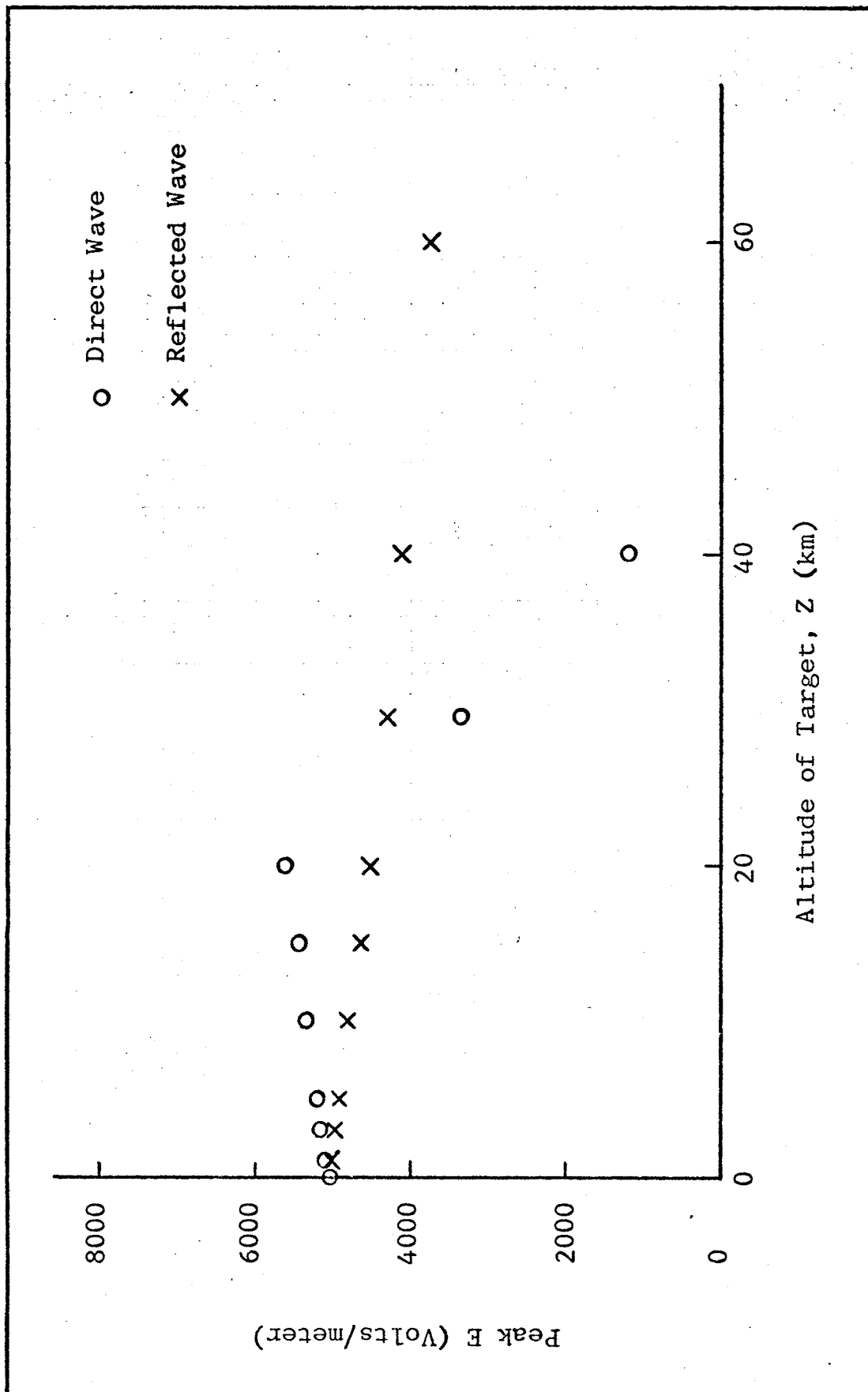


Fig. 8. Variation in Z Direction ( $X=0$ ,  $Y=+100\text{km}$ ,  $\gamma=.001\text{kt}$ ,  $\text{HOB}=100\text{km}$ )

region. Note that  $Y = 100$  km for these runs. As expected, the direct wave falls off rapidly as the target altitude passes through the absorption region, since less of the absorption region contributes to the wave with each increase in altitude. The crossover point where the reflected wave becomes the largest occurred at 25 km in this case. Above ground zero the crossover point was 29.4 km. The altitude of the crossover point is both yield and geometry dependent. It is necessary for the user to calculate both waves whenever there is any doubt which one is the largest.

The reflected wave calculation assumes 100% reflection from the ground and no attenuation in the absorption region or the ionosphere. These assumptions are reasonable if it is recalled that only the high frequency component is being considered and that it requires at least

$$\frac{40 \text{ km}}{3(10)^8 \text{ m/sec}} = 133 \text{ } \mu \text{ sec} \quad (67)$$

for the wave to leave the absorption region, reach the earth, be reflected, and return to the absorption region. This length of time is enough for a significant number of the free electrons to recombine and reduce the effective conductivity of the absorption region.

The results of variation in HOB are shown in Fig. 9. For all values of HOB attempted below 60 km the code went unstable. Infinite values for E were obtained which resulted in abnormal termination of the calculations. This is

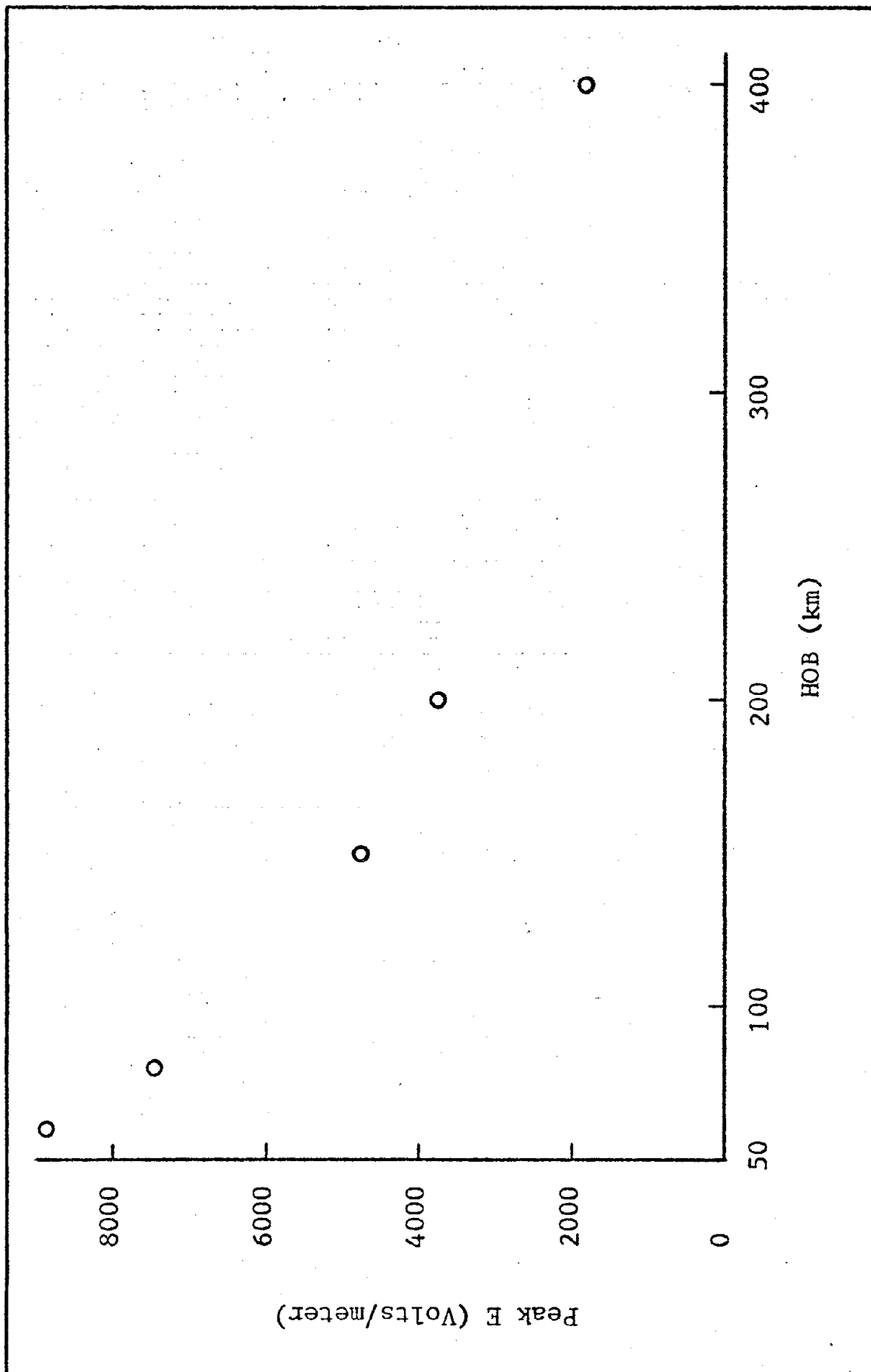


Fig. 9. Variation in Height of Burst ( $X=0$ ,  $Y=0$ ,  $Z=0$ ,  $Y_{\gamma}=0.001kt$ )

expected since the burst is assumed to be distant from the absorption region (equations 9 and 10).

The results of variation in gamma yield are shown in Fig. 10. For all gamma yields attempted above 60 tons the code went unstable, giving infinite values for E. However, the instability always occurred at times later than the natural peak value of E. For example, with 80 tons of gamma yield, the natural peak occurred at 1 shake and the instability occurred at 10 shakes. By using the natural peak value and ignoring the instability, reasonable values for peak E were obtained up to 1 kt of gamma yield.



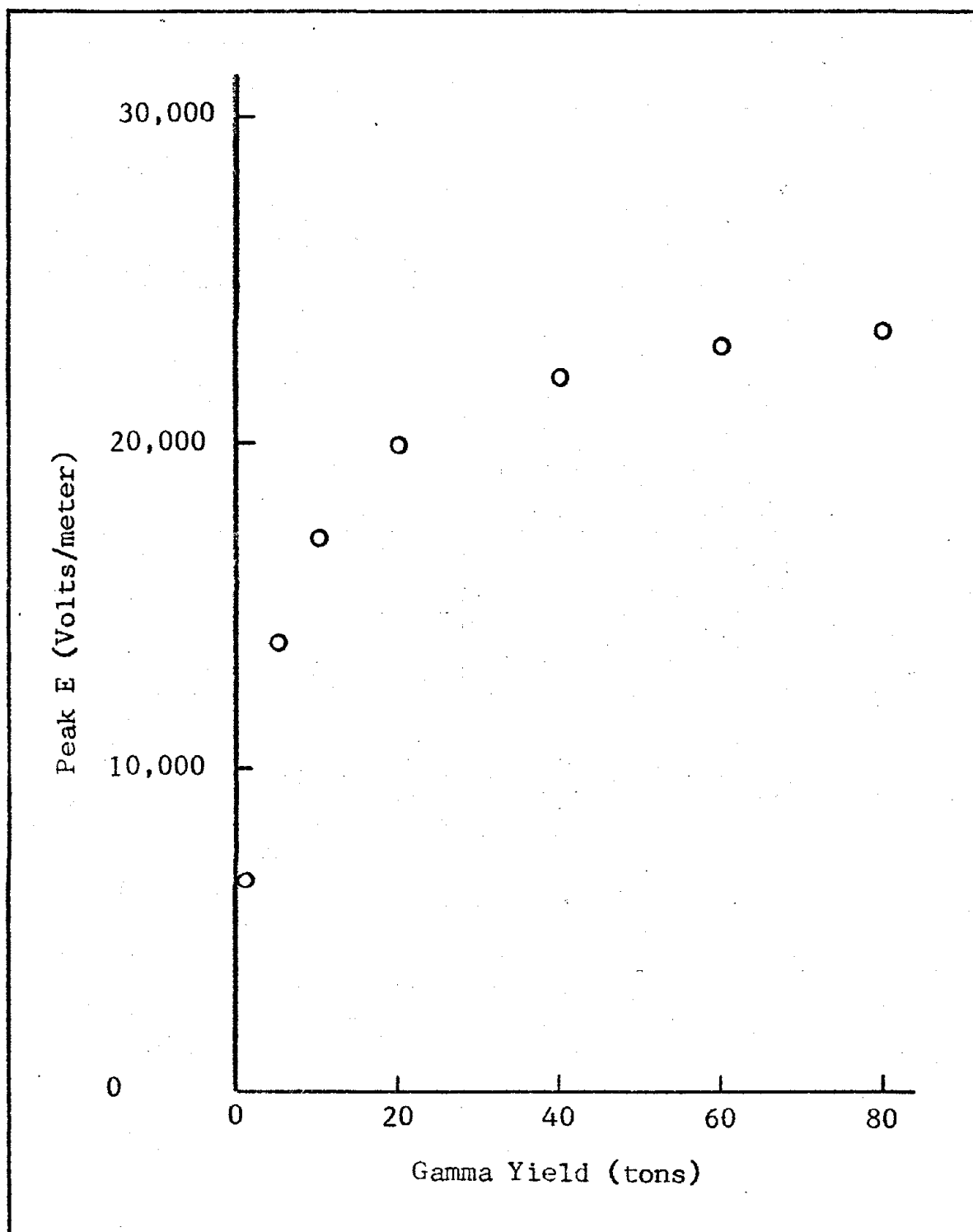


Fig. 10. Variation in Gamma Yield ( $X=0$ ,  $Y=0$ ,  $Z=0$ , HOB=100km)

## V. Discussion and Recommendations

### Limitations

Most of the limitations of the code are inherent in the model upon which it is based. Approximations such as a flat earth, a uniform magnetic field, and constant speed Compton electrons can be improved only by changing the model. In addition, the effect of the self generated electromagnetic fields on the motion of the Compton electrons is ignored, as is recombination of both primary and secondary electrons. The possibility of a single gamma ray interacting to produce more than one Compton electron is not allowed. In the absorption region the contribution of the non-propagating radial component of the electric field is neglected. Also, the model is not easily adapted to multi-group gamma transport, or to multiple burst calculations.

The code calculates only the effect of the gamma rays. The user must keep in mind that X-ray generated EMP becomes important for bursts above 100 km.

The code does not account for the increase in altitude of the absorption region for slant angles (angle A in Fig. 1) greater than  $60^\circ$  which is indicated by Latter and LeLevier (Ref 4).

Since 97% of the running time of the code is used for numerical iteration it is not practical to adapt the code to run more than one target at a time. Two targets would

merely double the running time, so it is simpler to just make two runs. Typical requirements are 200 seconds running time with 33000<sub>8</sub> words of central memory on the CDC 6600 computer using NDEL<sub>R</sub> = 50 and TMAX = 20 shakes.

### Uses

The code can be used to calculate the peak value of the E field at a target, anywhere on or above ground level, resulting from a nuclear burst above 60 km altitude with a gamma yield up to 60 tons. Either the direct or the ground reflected wave can be calculated. With special care, bursts up to 1 kt of gamma yield can be used.

### Recommendations

In the interest of accuracy, the targets should be located such that the slant angle,  $A$ , is between  $-60^\circ$  and  $+60^\circ$ .

By accepting a much longer running time the accuracy and hopefully, the stability of the code could be improved by using a smaller step size in the integration of the Compton current equations. Reducing the step size from one tenth of the Compton lifetime to one shake would require approximately ten times as much running time as the code presently requires. This possibility should be investigated further to determine the optimum step size for obtaining the best relationship between accuracy and running time.

Another possibility for increasing the accuracy and stability of the code is to reduce the step size in  $r$ . The present code has the capability of dividing the absorption region into 500 steps in  $r$  along the line of sight. Of course, the running time required for 500 steps is ten times that required for 50 steps. A modification of the code to allow more than 500 steps would increase the amount of computer core required as well as increasing the running time. This provides another area for investigation to determine the best trade off point between accuracy and running cost.

These two possibilities could be investigated with minor modifications to the present code. However, the computer time required would be considerable.

In addition, there are numerous possibilities for improvements in the model itself. Some of the more important ones are;

- Using multigroup gamma transport.

- Using multigroup Compton electrons.

- Allowing angular distribution of Compton electrons.

- Using self consistent electromagnetic fields.

- Including the low frequency components.

Each of these would require major modifications to the present code.

# Bibliography

1. Kinsley, O.V. Introduction to the Electromagnetic Pulse, Wright-Patterson AFB: Air Force Institute of Technology, March 1971. (GNE/PH/71-4).
2. Karzas, W. J. and R. Latter. "Detection of the Electromagnetic Radiation from Nuclear Explosions in Space", Physical Review, Vol 137, No. 5B. pages 1369-1378, March 8, 1965. (Also published as EMP Theoretical Note 40).
3. Pomranning, G. C. "Early Time Air Fireball Model for a Near-Surface Burst", DNA 3029T, March 1973.
4. Latter, R. and R. E. LeLevier. "Detection of Ionization Effects from Nuclear Explosions in Space", Journal of Geophysical Research, Vol. 68, No. 6, March 15, 1963.
5. Wylie, C. R. Jr. Advanced Engineering Mathematics, New York: McGraw-Hill Book Co. 1966. (Third Edition).
6. Lecture Notes, Electromagnetic Waves, EE 6.30, Air Force Institute of Technology, Wright-Patterson AFB, Summer, 1973. (Course taught by Maj. Carl T. Case.)

Appendix A

EMP Code User's Guide

EMP Code User's Guide

The code is run the same as any other Fortran Extended program, but due to the running time it should be converted to binary form before execution. The plotting subroutine requires an on-line plotter and both linear and log plotting library subroutines.

The input data is read in the following order:

Data card #1, using FORMAT (7F10.0, 215), contains;

X,Y,Z	The target coordinates in meters
HOB	The height of the burst in kilometers (60 km $\leq$ HOB)
GAMYLD	The gamma yield in kilotons (GAMYLD $\leq$ 1 kt)
BFIELD	The Earth's magnetic field in wb/m <sup>2</sup>
BANGLE	The magnetic field dip angle in degrees
NDELRL	The number of steps in r taken through the absorption region (50 $\leq$ NDELRL $\leq$ 500)
OUT	The output control parameter

Data card #2, using FORMAT (13), contains;

ITER	The time period covered by the iterations in shakes (10 $\leq$ ITER $\leq$ 100) (ITER = TMAX)
------	--

Data card #3, using FORMAT (4F10.0), contains;

A	Pomranning constant $\alpha$ in inverse shakes
B	Pomranning constant $\beta$ in inverse shakes
RN	Pomranning constant N in shakes
TO	Pomranning constant $\tau_0$ in shakes

Default values are provided for BANGLE, BFIELD, and NDELR. They are  $40^\circ$ ,  $0.00002 \text{ wb/m}^2$ , and 50 respectively. If these default values are desired, zero must be punched in their respective card fields.

The ground reflected wave at the target is obtained by reading in the target altitude, Z, as a negative number. For any target within the absorption region, both the direct and the ground reflected wave should be calculated to determine which one is the strongest.

For values of GAMYLD between 0.06 kilotons and 1.0 kilotons the code will most likely go unstable. This instability occurs after the real peak has been calculated, but the peak value printed out may not be the real peak. Since execution is terminated when the field becomes greater than  $1\text{E}15 \text{ V/m}$ , the array search can result in a false peak value. In this case, the array itself (or the plot) can be used to determine the real peak value.

Increasing NDELR makes the step size in r through the absorption region smaller and the calculation becomes more accurate. However, total running time varies directly with changes in NDELR. For example, using NDELR = 100 instead of NDELR = 50 will approximately double the running time required for NDELR = 50.

There are four output options provided. Option 0 prints out the informative messages, the calculated peak value at the target, the E array, and the  $\tau$  array. Option 1 adds a linear plot of the first 20 shakes and a log-log



plot of 100 shakes of E as a function of  $\tau$  at the target. Option 2 includes both Option 0 and Option 1 and adds a printout of E and  $\sigma$  as a function of  $\tau$  at the bottom of the absorption region. Option 3 deletes the plots from Option 2. The last two options are primarily for debugging since a partial printout is made for each completed iteration even if execution is terminated before the iterations are completed. The first two options are best for production runs.

The only requirements on the Pomranning constants are N must be chosen such that equations (61) and (62) are satisfied, all of them must be positive, and  $\alpha > \beta$ .

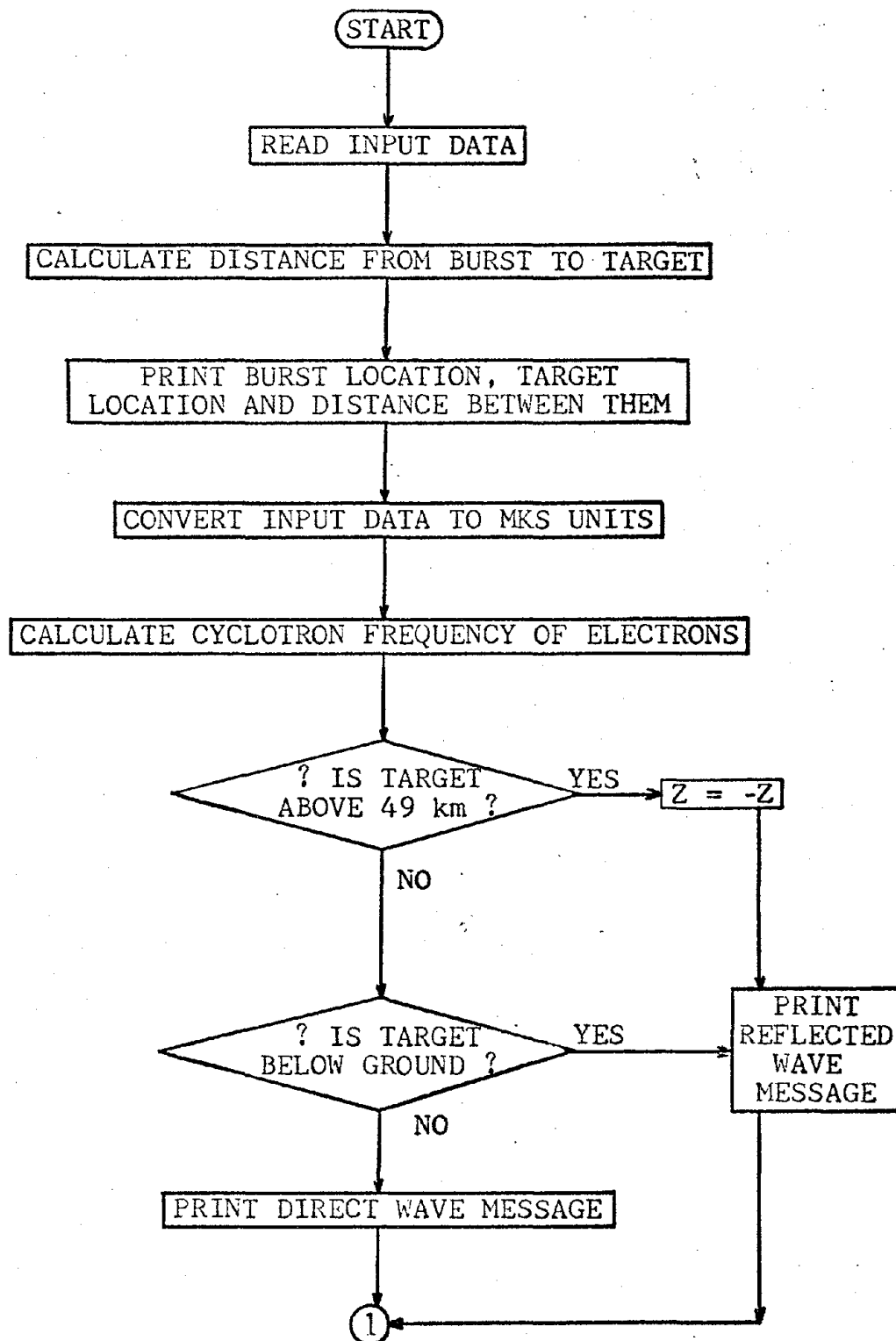
Increasing ITER also increases the running time. For ITER = 10 shakes, running time is approximately 180 seconds on the CDC 6600 computer. For ITER = 100 shakes, running time is approximately 340 seconds. A good compromise, which gives nice looking plots, is ITER = 20 shakes with a running time of approximately 200 seconds.

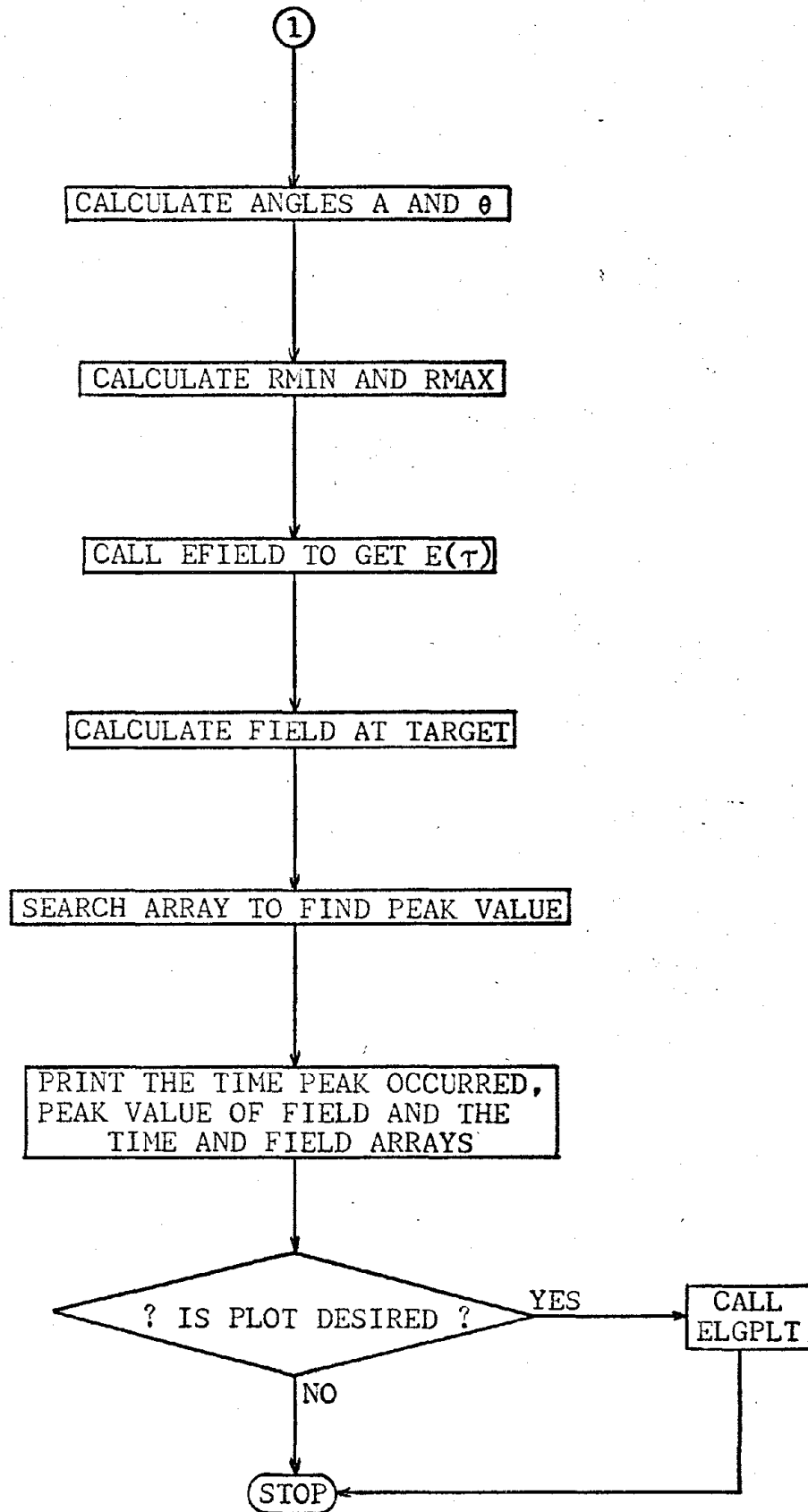
In binary form, the code requires  $33000_8$  words of core on the CDC 6600 computer.

Appendix B

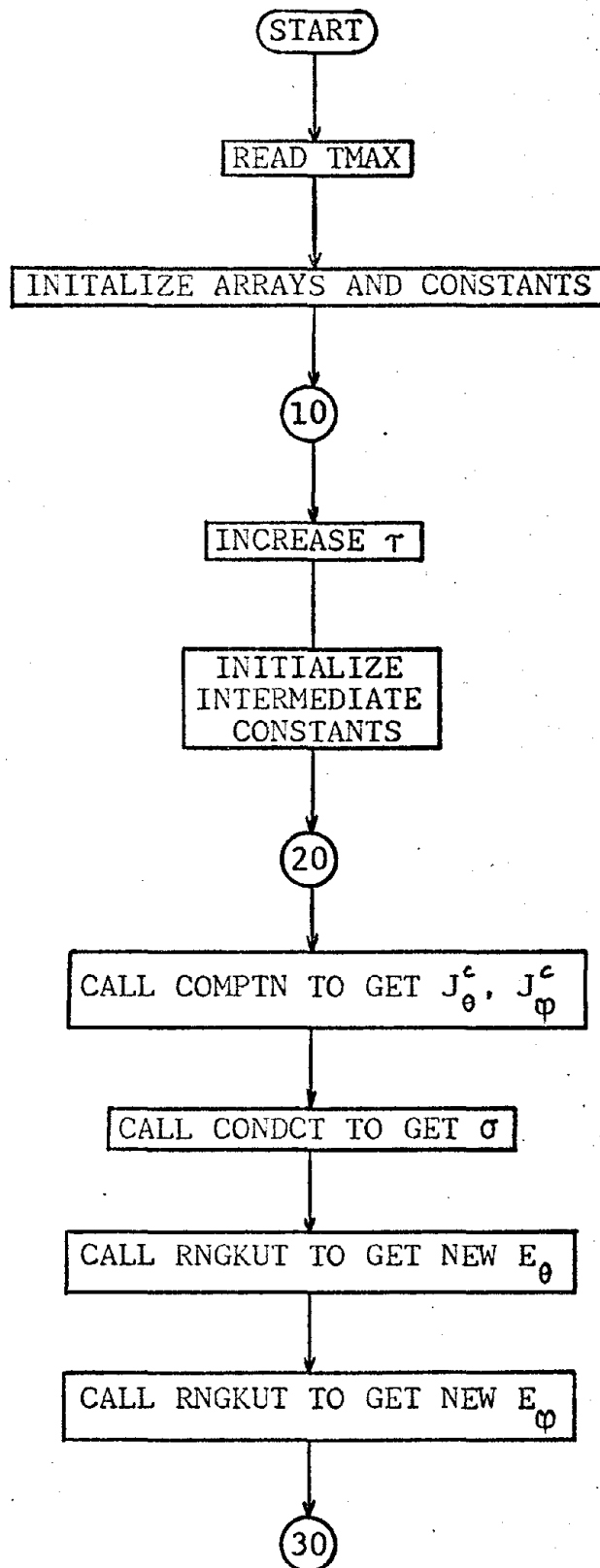
EMP Code Flow Charts

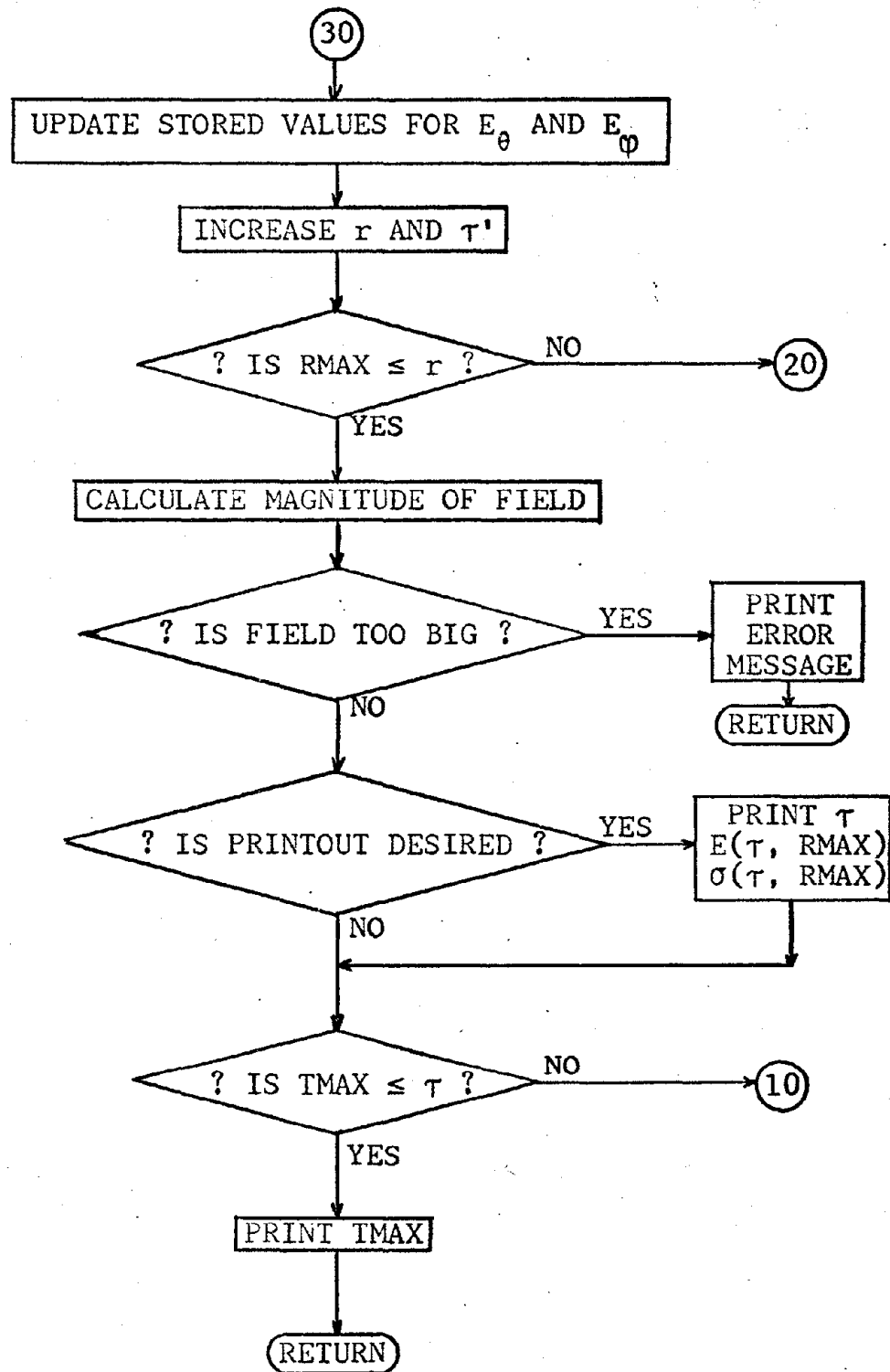
## PROGRAM CONTRL



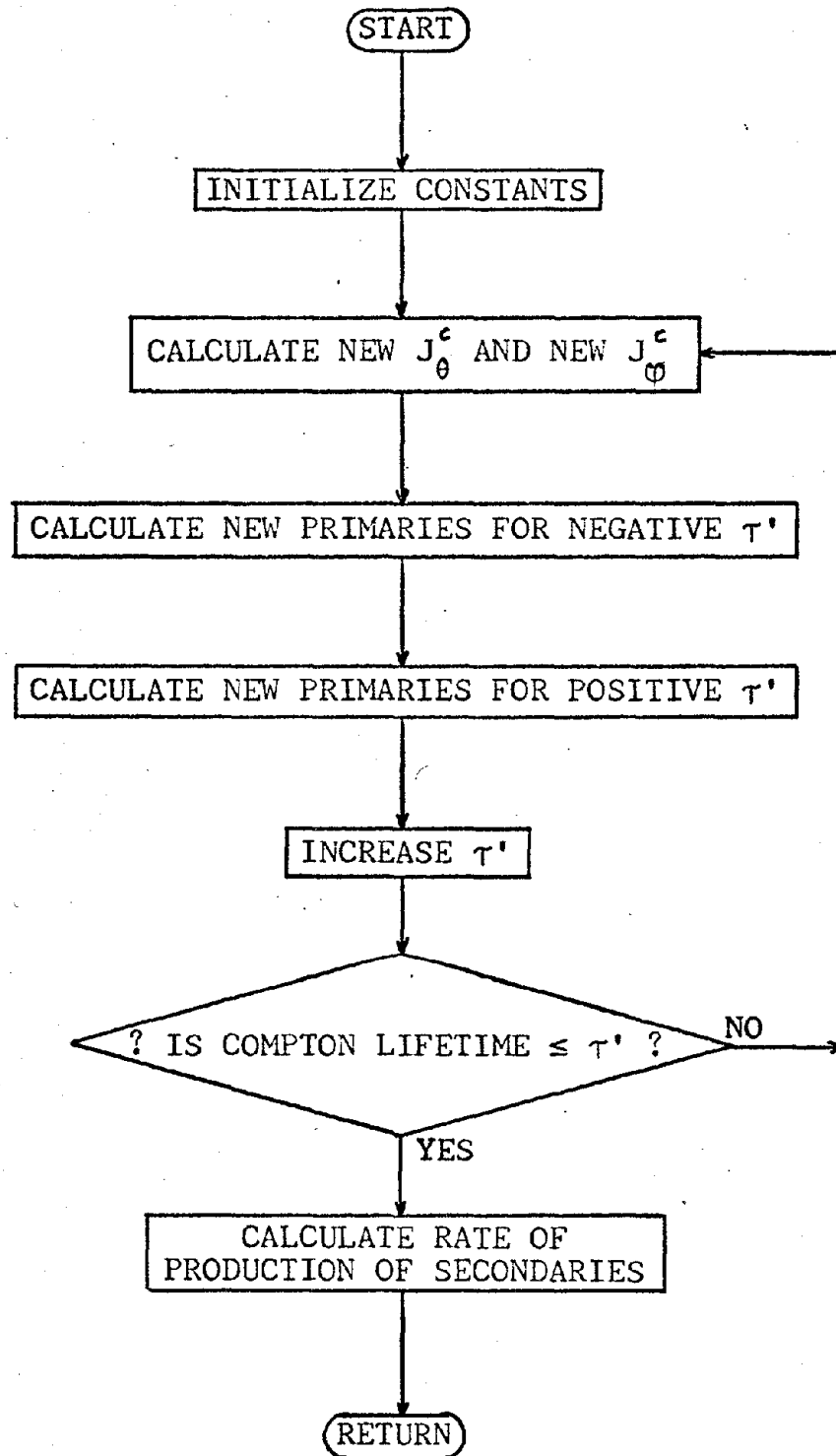


## SUBROUTINE EFIELD

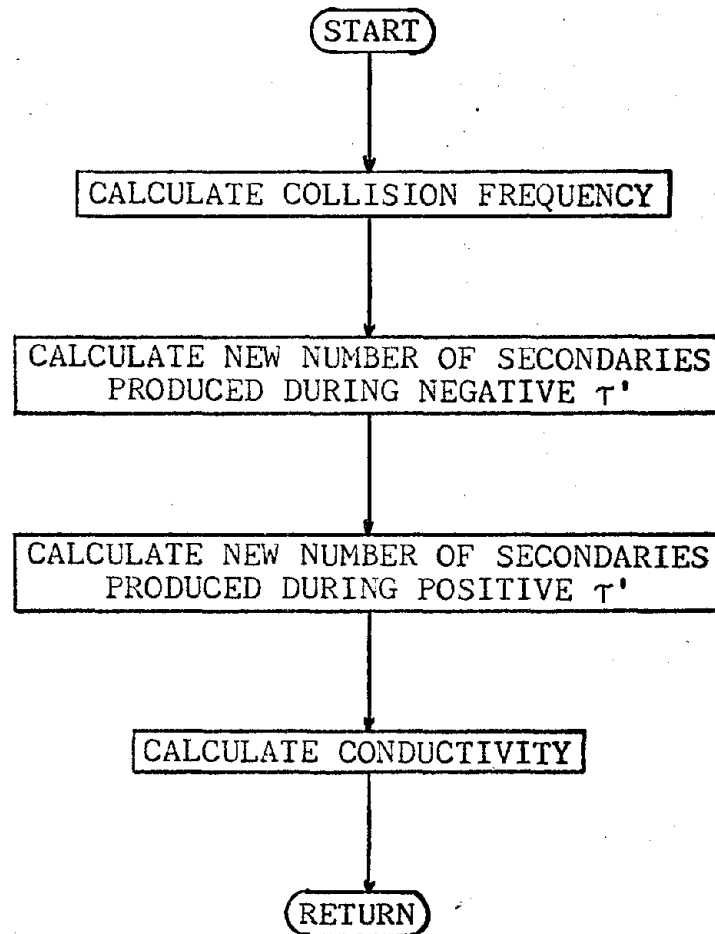




## SUBROUTINE COMPTN

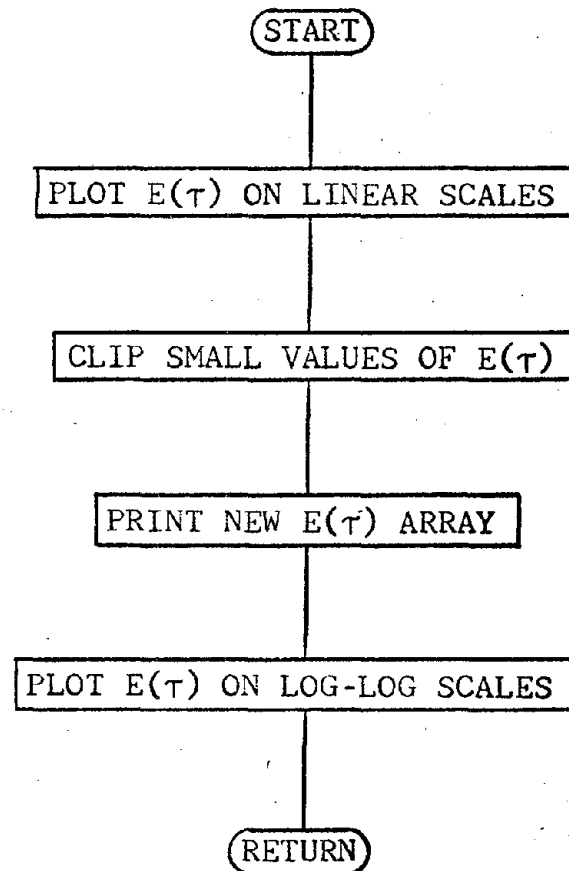


## SUBROUTINE CONDCT

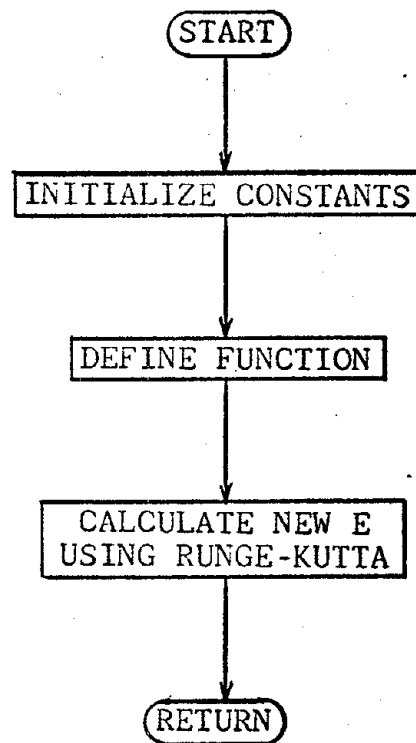




## SUBROUTINE ELGPLT



SUBROUTINE RNGKUT



Appendix C

EMP Code Listing

6

```

C      SET UP DEFAULT VALUES
C
C      IF(BANGLE.EQ.0.) BANGLE=40.
C      IF(RFIELD.EQ.0.) RFIELD=0.00002
C      IF(NDELR.EQ.0) NDELR=50
C
C      CONVERT DATA TO MKS UNITS
C
C      HCR=HOB*1000.
C      GAMYLD=2.61625E25*GAMYL
C      BANGLE=0.017453295*BANGLE
C      OMEGA=1.6E-19*BFIELD/(3.505*9.11E-31)
C
C      PRINT TYPE OF CALCULATION
C
C      REFLCT=49000.
C      IF(Z.GT.REFLCT)PRINT 2007
C      IF(Z.LT.0.0) PRINT 2008
C      IF(Z.LE.REFLCT.AND.Z.GE.0.0) PRINT 2009
C
C      REFLECTED WAVE CALCULATION ASSUMES 100% REFLECTION
C      AND USES MIRROR IMAGE OF TARGET BELOW GROUND
C      SET Z = -Z IF REFLECTED WAVE IS TO BE USED
C
C      IF(Z.GT.REFLCT) Z=-Z
C      IF(Z.GT.HOB-1000.) PRINT 2007
C      IF(Z.GT.HOB-1000.) Z=-Z
C
C      DETERMINE ANGLES
C
C      R=SQRT(X*X+Y*Y+(HOB-Z)**2)
C      A=ACOS((HOB-Z)/R)
C      THETA=ACOS(COS(BANGLE)*Y/R+SIN(BANGLE)*(Z-HOB)/R)
C
C      DETERMINE RMIN AND RMAX
C
CNTL 370
CNTL 380
CNTL 390
CNTL 400
CNTL 410
CNTL 420
CNTL 430
CNTL 440
CNTL 450
CNTL 460
CNTL 470
CNTL 480
CNTL 490
CNTL 500
CNTL 510
CNTL 520
CNTL 530
CNTL 540
CNTL 550
CNTL 560
CNTL 570
CNTL 580
CNTL 590
CNTL 600
CNTL 610
CNTL 620
CNTL 630
CNTL 640
CNTL 650
CNTL 660
CNTL 670
CNTL 680
CNTL 690
CNTL 700
CNTL 710
CNTL 720

```

```

ZRMIN=5.E4
IF(HOB.LT.ZRMIN) ZRMIN=HCE
TA=((ZRMIN-HOB)/(Z-HOB)
XRMIN=TA*X
YRMIN=TA*Y
RMIN=SQRT(XRMIN**2+YRMIN**2+(ZRMIN-HOB)**2)
ZRMAX=Z
IF(Z.LT.2.E4) ZRMAX=2.E4
TB=((ZRMAX-HOB)/(Z-HOB)
XRMAX=TB*X
YRMAX=TB*Y
RMAX=SQRT(XRMAX**2+YRMAX**2+(ZRMAX-HOB)**2)

      CALCULATE EFIELD AT ECITCM OF ABSORFTION REGION

CALL EFIELD(E,TIME,RMIN,RMAX,NDELR,HOB,A,THETA,OMEGA,GAMYL,C,
1STORE2)

      CALCULATE EFIELD AT TARGET

IF(R.LE.RMAX) GO TO 3
DO 1 I=1,190
E(I)=E(I)*RMAX/R

      FIND PEAK VALUE OF EFIELD

PIG=0.0
DO 2 I=1,190
IF(E(I).GT.BIG) 4,2
BIG=E(I) $ IT=I
CONTINUE

      PRINT OUTPUT

PRINT 2010,TIME(IT)
PRINT 2005,BIG

```

```

CNTL 730
CNTL 740
CNTL 750
CNTL 760
CNTL 770
CNTL 780
CNTL 790
CNTL 800
CNTL 810
CNTL 820
CNTL 830
CNTL 840
CNTL 850
CNTL 860
CNTL 870
CNTL 880
CNTL 890
CNTL 900
CNTL 910
CNTL 920
CNTL 930
CNTL 940
CNTL 950
CNTL 960
CNTL 970
CNTL 980
CNTL 990
CNTL1000
CNTL1010
CNTL1020
CNTL1030
CNTL1040
CNTL1050
CNTL1060
CNTL1070
CNTL1080

```



```

C C C C
SUBROUTINE EFIELD(E,TIME,RMIN,RMAX,NDELR,HOB,A,THETA,OMEGA,GAMMYLJ,
1STORE2)
EFLD 10
EFLD 20
EFLD 30
EFLD 40
EFLD 50
EFLD 60
EFLD 70
EFLD 80
EFLD 90
EFLD 100
EFLD 110
EFLD 120
EFLD 130
EFLD 140
EFLD 150
EFLD 160
EFLD 170
EFLD 180
EFLD 190
EFLD 200
EFLD 210
EFLD 220
EFLD 230
EFLD 240
EFLD 250
EFLD 260
EFLD 270
EFLD 280
EFLD 290
EFLD 300
EFLD 310
EFLD 320
EFLD 330
EFLD 340
EFLD 350
EFLD 360

C C C C
      CALCULATE THE EFIELD IN THE ABSORPTION REGION

C C C C
      DIMENSION E(190),TIME(190),STORE2(NDELR)
      REAL JTHETA,JPHI
      INTEGER OUT
      COMMON OUT,AP,BP,RNP,TOP

C C C C
      ITER IS TIME OF ITERATION IN SHAKES 10<=ITER<=100
      READ ITER AND CHANGE IT TO NUMBER OF TIME STEPS

C C C C
      READ 100,ITER
      ITER=100+(ITER-10)

C C C C
      INITIALIZE ARRAYS AND CONSTANTS

C C C C
      READ 101,AP,BP,RNP,TOP
      FORMAT(4F10.0)
      DO 51 J=1,100
      E(J)=0.0 $ TIME(J)=0.1*J
51 CONTINUE
      DO 71 J=101,190
      E(J)=0.0 $ TIME(J)=1.0+(J-100.)
71 CONTINUE
      DO 51 L=1,NDELR $ STORE2(L)=0.
51 CONTINUE
      ETHE=0. $ DELRN=NDELR $ T=0. $ OF=1. $ EPHI=0.
      DELTAR=(RMAX-RMIN)/DELRN $ R=RMIN+DELTAR $ RNP=1.E-3*RNP

C C C C
      START INTEGRATIONS
      OUTSIDE LOOP IS FOR CALCULATION IN RETARDED TIME
      INSIDE LOOP IS FOR INTEGRATION IN R AT EACH TIME STEP

```



```
CC 21 I=1,190 $ T=T+(1.E-9)*CT $ TIME(I)=T*(1.E8) EFLLC 370
IT=I EFLLC 380
IF(I.GT.ITER) GO TO 42 EFLLC 390
TP=-DELTAR/2.88E8$ CTP=TF $ SIGMA=0.$ STORE1=0. EFLLC 400
CO 31 K=1,NDEL R EFLLC 410
CALL CCMPFN(JTHETA,JPHI,I,R,A,THETA,OMEGA,PCB,GAMYLD,TP,PRI,FRI2) EFLLC 420
CALL CCNDOCT(SIGMA,FRI,CTF,CI,HOB,R,A,SICRE1,STORE2,K,NDELR,FRI2) EFLLC 430
CALL RNGKUT(ETHENW,ETHE,R,CELTAR,SIGMA,JTHETA) EFLLC 440
CALL RNGKUT(EPHINW,EPhi,R,CELTAR,SIGMA,JPHI) EFLLC 450
ETHE=ETHENW $ EPHI=EPhinw $ F=R+DELTAR EFLLC 460
TP=TP+CTP EFLLC 470
CONTINUE EFLLC 480
EFLLC 490
EFLLC 500
EFLLC 510
EFLLC 520
EFLLC 530
EFLLC 540
EFLLC 550
EFLLC 560
EFLLC 570
EFLLC 580
EFLLC 590
EFLLC 600
EFLLC 610
EFLLC 620
EFLLC 630
EFLLC 640
EFLLC 650
EFLLC 660
EFLLC 670
EFLLC 680
EFLLC 690
EFLLC 700
EFLLC 710
EFLLC 720

          FIND MAGNITUDE OF EFIELD
          CHECK FOR DIVERGENCE OF SOLUTION
          IF DESIRED, PRINT OUTPLT
          IF (OUT-1.LE.0) GO TO 21
          PRINT 5,I,TIME(I),E(I),SIGMA
          CONTINUE
          PRINT MESSAGE AFTER TERMINATION OF TIME LOOP
          PRINT 201,TIME(ITER)
          RETURN
          PRINT MESSAGE AFTER AERONORMAL TERMINATION OF TIME LOOP
```

EFLC 730  
EFLC 740  
EFLC 750  
EFLC 760  
EFLC 770  
EFLC 780  
EFLC 790  
EFLC 800  
EFLC 810  
EFLC 820  
EFLC 830  
EFLC 840  
EFLC 850  
EFLC 860  
EFLC 870

```

52      PRINT 301
      PRINT 201, TIME(IT)
      IF(IT.LT.10) RETURN
C
C      SET LAST 5 VALUES OF EFIELD TO 0.0 TO AVOID INCORRECT PEAK
C
      E(IT)=E(IT-1)=E(IT-2)=E(IT-3)=E(IT-4)=E(IT-5)=0.0
      RETURN
100     FORMAT (I3)
5       FORMAT (" I =", I4, "      TIME =", F6.1, " SHAKES      E(T,RMAX) =",
11PE10.3, " VOLTS/METER      SIGMA =", 1PE10.3, " MHO/METER")
201     FORMAT (//5X, "ITERATION TERMINATED AFTER", F5.1, " SHAKES"//)
301     FORMAT (//15X, "*****"/15X, "***** SOLUTION HAS GONE UNSTABLE"
1/15X, "*****"//)
      END

```

CNDT 10  
CNDT 20  
CNDT 30  
CNDT 40  
CNDT 50  
CNDT 60  
CNDT 70  
CNDT 80  
CNDT 90  
CNDT 100  
CNDT 110  
CNDT 120  
CNDT 130  
CNDT 140  
CNDT 150  
CNDT 160

```

SUBROUTINE CCNDCT(SIGMA, FFI, CTP, DT, HOB, R, A, STORE1, STORE2, K, NDEL,
1PRI2)
C
C      CALCULATES SIGMA AFTER FINDING
C      NSECONDARY FROM NPRIMARY
C
C      STORE1 CCNTAINS INTEGRAL FOR NEGATIVE TAU
C      STORE2 CCNTAINS INTEGRAL FOR POSITIVE TAU
C
      DIMENSION STORE2(NDEL)
      CCLISN=4.E12*EXP((R*CCOS(A)-PCB)/7000.)
      STORE1=STORE1-PRI*CTP
      STORE2(K)=STORE2(K)+PRI2*CT*(1.0E-9)
      SEC=STORE2(K)-STORE1
      SIGMA=(1.6E-19**2)*SEC/(CCLISN*9.11E-31)
      RETURN $ END

```

```

SUBROUTINE CCMPIN(JTHETA,JPHI,T,R,A,THETA,CMEGA,HOB,GAMYLD,TF,FRI,CMTN 10
1PRI2) CMTN 20
CMTN 30
CMTN 40
CMTN 50
CMTN 60
CMTN 70
CMTN 80
CMTN 90
CMTN 100
CMTN 110
CMTN 120
CMTN 130
CMTN 140
CMTN 150
CMTN 160
CMTN 170
CMTN 180
CMTN 190
CMTN 200
CMTN 210
CMTN 220
CMTN 230
CMTN 240
CMTN 250
CMTN 260
CMTN 270
CMTN 280
CMTN 290
CMTN 300
CMTN 310
CMTN 320
CMTN 330
CMTN 340
CMTN 350
CMTN 360

      CALCULATE THE TWO COMPONENTS OF THE
      COMPTON CURRENT AT GIVEN T AND R
      CALCULATE NUMBER OF PRIMARY ELECTRONS

      JTHETA IS THETA COMPONENT OF COMPTON CURRENT
      JPHI IS PHI COMPONENT OF COMPTON CURRENT
      TMAX IS COMPTON LIFETIME
      PATH IS ALTITUDE SCALFC COMPTON MEAN FREE PATH
      TP IS NEGATIVE RETARDED TIME
      T IS POSITIVE RETARDED TIME
      PRI IS NUMBER OF PRIMARY ELECTRONS GENERATED DURING TF
      PRI2 IS NUMBER OF PRIMARY ELECTRONS GENERATED DURING T
      TPRIME IS VARIABLE OF INTEGRATION

      INITIALIZE CONSTANTS

      REAL JTHETA,JPHI
      JTHETA=0. $ JPHI=0. $ TPRIME=(5.E-9) $ TMAX=CLIFE(R,A,HOB)$FRI=0.
      DT=TMAX/10. $ PATH=309.*EXP(-(HOB-R*COS(A))/7000.)$TPRIME=DT$W=DT/2.
      PRI2=0.

      RUNGE-KUTTA INTEGRATION OF COMPTON CURRENT

      DO 31 K=1,10
      RK1=DT*CMTHET(HOB,R,A,THETA,CMEGA,PATH,T,TPRIME,GAMYLD)
      RK2=DT*CMTHET(HOB,R,A,THETA,CMEGA,PATH,T,TPRIME+W,GAMYLD)
      RK3=RK2
      RK4=DT*CMTHET(HOB,R,A,THETA,CMEGA,PATH,T,TPRIME+DT,GAMYLD)
      JTHETA=JTHETA+(RK1+2.*(RK2+RK3)+RK4)/6.
      RK5=DT*CMPHI(HOB,R,A,THETA,CMEGA,PATH,T,TPRIME,GAMYLD)
      RK6=DT*CMPHI(HOB,R,A,THETA,CMEGA,PATH,T,TPRIME+W,GAMYLD)
      RK7=RK6
      RK8=DT*CMPHI(HOB,R,A,THETA,CMEGA,PATH,T,TPRIME+DT,GAMYLD)

```

```

JPHI=JPHI+(RK5+2.*(RK6+RK7)+RK8)/6.
      RUNGE-KUTTA INTEGRATION OF PRIMARIES
      RKP1=DT*RKCMTN(R,THETA,OMEGA,TP,TPRIME)
      RKP2=DT*RKCMTN(R,THETA,OMEGA,TP,TPRIME+W)
      RKP3=RKP2
      RKP4=DT*RKCMTN(R,THETA,OMEGA,TP,TPRIME+DT)
      PRI=PRI+(RKP1+2.*(RKP2+RKP3)+RKP4)/6.
      RP1=DT*RKCMTN(R,THETA,CMEGA,T,TPRIME)
      RP2=DT*RKCMTN(R,THETA,OMEGA,T,TPRIME+W)
      RP3=RP2
      RP4=DT*RKCMTN(R,THETA,CMEGA,T,TPRIME+DT)
      PRI2=PRI2+(RP1+2.*(RP2+RP3)+RP4)/6.
      TPRIME=TPRIME+DT
      CONTINUE
      MULTIPLY PRIMARIES BY Q*G(R)/TMAX
      TO OBTAIN RATE OF PRODUCTION OF SECONDARIES
      PRI=PRI*5.000E4*GOFR(R,A,HOB,PATH,GAMYLD)/TMAX
      PRI2=PRI2*5.0E4*GOFR(R,A,HOB,PATH,GAMYLD)/TMAX
      RETURN $ END

```

C  
C  
C

31

C  
C  
C  
C

```

FUNCTION CMPHI(HOB,P,A,THETA,OMEGA,PATH,T,TPRIME,GAMYLD)
      CALCULATES F(T,P) FOR RUNGE-KUTTA INTEGRATION
      OF PHI COMPONENT OF CMFTON CURRENT
      SOLVE=TOFT(T,TPRIME,THETA,CMEGA)
      SOLVE=FOFT(SOLVE)
      SOLVE=SOLVE*(-4.608E-11)*GCFF(R,A,HOB,PATH,GAMYLD)
      CMPHI=SOLVE*SIN(THETA)*SIN(OMEGA*TPRIME)
      RETURN $ END

```

```

CMPH11010
CMPH11020
CMPH11030
CMPH11040
CMPH11050
CMPH11060
CMPH11070
CMPH11080
CMPH11090
CMPH11100

```

C  
C  
C  
C

```

FUNCTION CMTHET(HOB,R,A,THETA,OMEGA,PATH,T,TPRIME,GAMYLD)
      CALCULATES F(T,P) FOR RUNGE-KUTTA INTEGRATION
      OF THETA COMPONENT OF CMFTON CURRENT
      SOLVE=TOFT(T,TPRIME,THETA,CMEGA)
      SOLVE=FOFT(SOLVE)
      SOLVE=SOLVE*(-4.608E-11)*GCFF(R,A,HOB,PATH,GAMYLD)
      CMTHET=SOLVE*SIN(THETA)*COS(OMEGA*TPRIME)-1.
      RETURN $ END

```

```

CMTH11010
CMTH11020
CMTH11030
CMTH11040
CMTH11050
CMTH11060
CMTH11070
CMTH11080
CMTH11090
CMTH11100

```

C  
C  
C  
C

RNKT1010  
RNKT1020  
RNKT1030  
RNKT1040  
RNKT1050  
RNKT1060  
RNKT1070  
RNKT1080  
RNKT1090  
RNKT1100  
RNKT1110  
RNKT1120  
RNKT1130

SUBROUTINE RNGKIIT (L1,E,F,T,SIGMA,COMPTJ)

C  
C  
C  
C

E(I+1) IS CALCULATED FROM E(I)  
USING THE RUNGE-KUTTA METHOD

DATA (C=3.0E8), (RMUC=12.56637E-7)  
EFUN(R,E)=- (1./R+C\*FMUO\*SIGMA/2.)\*E-COMPTJ\*C\*RMUO/2.  
RK1=H\*EFUN(R,E)  
RK2=H\*EFUN(R+H/2.,E+RK1/2.)  
RK3=H\*EFUN(R+H/2.,E+RK2/2.)  
RK4=H\*EFUN(R+H,E+RK3)  
E1=E+(RK1+2.\*(RK2+RK3)+RK4)/6.  
RETURN \$ END

RKCP1010  
RKCP1020  
RKCP1030  
RKCP1040  
RKCP1050  
RKCP1060  
RKCP1070  
RKCP1080

FUNCTION RKCMTN(R,THETA,CMEGA,TP,TPRIME)

C  
C  
C  
C

CALCULATES F(T) FOR RUNGE-KUTTA  
INTEGRATION OF PRIMARY ELECTRONS

SOLVE=TOFT(TF,TPRIME,THETA,CMEGA)  
RKCMTN=FCFT(SOLVE)  
RETURN \$ END

GCFR1010  
GOFR1020  
GCFF1030  
GCFF1040  
GOFR1050  
GCFF1060  
GOFR1070  
GCFF1080  
GOFR1090

FUNCTION GOFR (R,A,HOP,FATH,GAMYLD)

SOLVES VIRGIN TRANSFCRT AND USES REACTION RATE TO  
CALCULATE THE NUMBER DENSITY OF RACIAL ELECTRONS

SOLVE=(.0226275/COS(A))\*(-1.+EXP(R\*COS(A)/7000.))\*EXP(-HOB/7000.)  
DENOM=12.56637\*R\*R\*FATH\*1.E  
GCFR=EXP(-SOLVE)\*GAMYLD/CENCM  
RETURN \$ END

C  
C  
C  
C

CLIF1010  
CLIF1020  
CLIF1030  
CLIF1040  
CLIF1050  
CLIF1060  
CLIF1070  
CLIF1080  
CLIF1090

FUNCTION CLIFE (R,A,HOP)

CALCULATES COMPTON LIFETIME AT RADIUS = R  
MAX ACCEPTABLE LIFETIME = 100 SHAKES FCR  
THE KARZAS-LATTER HIGH FREQUENCY APPROX

CLIFE=1.041667E-8\*EXP((-CE-R\*COS(A))/7000.)  
IF(CLIFE.GT.1.E-6) CLIFE=(1.E-6)  
RETURN \$ END

C  
C  
C  
C  
C

TOFT1010  
TOFT1020  
TOFT1030  
TOFT1040  
TOFT1050  
TOFT1060  
TOFT1070  
TOFT1080  
TOFT1090

```

FUNCTION TOFT (T,TPRIME,THETA,OMEGA)
      T(T) IS TIME TRANSFORMED TO KARZAS-LATTER FORM
      B=0.958
      FIRST=T-(1.-B*(COS(THETA)**2))*TPRIME
      SECOND=B*(SIN(THETA)**2)*SIN(OMEGA*TPRIME)/OMEGA
      TOFT=FIRST+SECOND
      RETURN $ END

```

C  
C  
C

FOFT1010  
FOFT1020  
FOFT1030  
FOFT1040  
FOFT1050  
FOFT1060  
FOFT1070  
FOFT1080  
FOFT1090  
FOFT1100  
FOFT1110

```

FUNCTION FOFT(T)
      F(T) IS THE POMRANNING MODEL FOR TIME DEPENDENCE
      OF NUCLEAR WEAPON YIELD IN RETARDED TIME
      INTEGER OUT
      COMMON OUT,A,B,RN,T
      TSHAKE=1.E8*T
      DENOM=(B+A*EXP((A+B*(TSHAKE-T))))*RN
      FOFT=(A+B)*EXP(A*(TSHAKE-T))/DENOM
      RETURN $ END

```

C  
C  
C  
C



```

C
C
C
SUBROUTINE ELGPLT(EFLOT,TIME,BIG)
    THE FIRST 20 SHAKES OF E(T) IS PLOTTED ON LINEAR SCALES
    DIMENSION EFLOT(192),TIME(192),E(112),T(112)
    MAG = 5 & SMALL = 0.0
    CHECK = 0.0
    DO 6 I=1,110
        E(I)=EFLOT(I) & T(I)=TIME(I)
    CCNTINUE
    CALL PLOT (0.0,-8.0,-3)
    CALL PLOT (2.0,2.0,-3)
    CALL SCALE (T,5.,110,1)
    CALL SCALE (E,5.,110,1)
    CALL LINE(T,E,110,1,0,0)
    CALL AXIS(0.,0.,13*TIME (SPAKES),-13,5.,0.,T (111),T (112))
    CALL AXIS(0.,0.,12*HEFIELD (V/M),12,5.,90.,E (111),E (112))
    CALL AXIS(0.,5.,2H,2,5.,0.,T (111),T (112))
    CALL AXIS(5.,0.,2H,-2,5.,90.,E (111),E (112))
    CALL PLOT(10.0,2.0,-3)
    SMALL VALUES OF E(T) ARE CLIPPED OFF
    AND E(T) IS PLOTTED ON LOG-LOG SCALES
    DO 3 I=1,190
        IF((EFLOT(I)/BIG).LT.(10.*(-MAG)))2,3
        EFLOT(I)=BIG*(10.*(-MAG)) & CHECK=1.
    CCNTINUE
    IF(CHECK.EQ.0.) GO TO 11
    PRINT 2005
    PRINT 2006,(EFLOT(I),I=1,190)
    SMALL=BIG*(10.*(-MAG))
    PRINT 2007,SMALL,BIG
    CCNTINUE
    CALL PLOT (0.0,-8.0,-3)
    CALL PLOT (2.0,2.0,-3)

```

EPLT 10  
EPLT 20  
EPLT 30  
EPLT 40  
EPLT 50  
EPLT 60  
EPLT 70  
EPLT 80  
EPLT 90  
EPLT 100  
EPLT 110  
EPLT 120  
EPLT 130  
EPLT 140  
EPLT 150  
EPLT 160  
EPLT 170  
EPLT 180  
EPLT 190  
EPLT 200  
EPLT 210  
EPLT 220  
EPLT 230  
EPLT 240  
EPLT 250  
EPLT 260  
EPLT 270  
EPLT 280  
EPLT 290  
EPLT 300  
EPLT 310  
EPLT 320  
EPLT 330  
EPLT 340  
EPLT 350  
EPLT 360

71

```

CALL LGSCAL (TIME,5.0,190)
CALL LGSCAL (EPLT,5.0,190)
CALL LGLINE (TIME,EPLT,190,C,0,0)
CALL LGAXIS(0.,0.,13*TIME (SFACES),-13,5.,0.,TIME(191),TIME(192))
CALL LGAXIS(0.,0.,12*HEFIELD (V/M),12,5.,90.,EPLT(191),EPLT(192))
CALL LGAXIS(0.,5.,2H ,2,5.,0.,TIME(191),TIME(192))
CALL LGAXIS(5.,0.,2H , -2,5.,90.,EPLT(191),EPLT(192))
CALL PLOTE
RETURN
2005 FCRMAT("1 * * WARNING: FLOT OF E(T) HAS BEEN CLIPPED * * *")EPLT 460
2006 FCRMAT(/5X,"CLIPPED E(T) IS"//19(10(3X,1PE10.3)/))EPLT 470
2007 FCRMAT(//" MINIMUM E(T) IS",1PE10.3/" MAXIMUM E(T) IS",1PE10.3EPLT 480
1)EPLT 490
END
EPLT 500

```

Vita

Terry C. Chapman was born on 21 August 1943 in Vancouver, Washington. He graduated from high school in Manitou Springs, Colorado in 1961. He attended the University of Colorado in Boulder where he was elected to Tau Beta Pi, Engineering Honor Society and Sigma Pi Sigma, Physics Honor Society. He received the degree Bachelor of Science, Engineering Physics and a commission in the U. S. Air Force from the University of Colorado in 1969. After attending communications training, he was assigned to Kelly AFB, Texas as a communications operations officer in 1970. He entered the Air Force Institute of Technology in 1972.

Permanent Address: P.O. Box 1144

Manitou Springs, Colorado 80829

This thesis was typed by Ladonna Stitzel.